

# Apoptotic cells promote circulating tumor cell survival and metastasis

Cassidy Hagan

A dissertation

submitted in partial fulfillment of the  
requirements for the degree of

Doctor of Philosophy

University of Washington

2024

Reading Committee:

Andrew Oberst, Chair

Kevin Urdahl

Mark Headley

Program Authorized to Offer Degree:

Immunology

© Copyright 2024

Cassidy Hagan

University of Washington

**Abstract**

**Apoptotic cells promote circulating tumor cell survival and metastasis**

Cassidy Hagan

Chair of the Supervisory Committee:

Andrew Oberst

Department of Immunology

During tumor progression and especially following cytotoxic therapy, cell death of both tumor and stromal cells is widespread. Despite clinical observations that high levels of apoptotic cells correlate with poorer patient outcomes, the physiological effects of dying cells on tumor progression remain incompletely understood. Here, we report that circulating apoptotic cells robustly enhance tumor cell metastasis to the lungs. Using intravenous metastasis models, we observed that the presence of apoptotic cells, but not cells dying by other mechanisms, supports circulating tumor cell (CTC) survival following arrest in the lung vasculature. Apoptotic cells promote CTC survival by recruiting platelets to the forming metastatic niche. Apoptotic cells externalize the phospholipid phosphatidylserine to the outer leaflet of the plasma membrane, which we found increased the activity of the coagulation initiator Tissue factor, thereby triggering the formation of platelet clots that protect proximal CTCs. Inhibiting the ability of apoptotic cells to induce coagulation by knocking out Tissue factor, blocking phosphatidylserine, or administering the anticoagulant heparin abrogated the pro-metastatic effect of apoptotic cells. This work demonstrates a previously unappreciated role for apoptotic cells in facilitating metastasis by establishing CTC-supportive emboli, and suggests points of intervention that may reduce the pro-metastatic effect of apoptotic cells.

# Table of Contents

Table of Contents .....	i
List of Figures .....	ii
List of Abbreviations .....	iii
Acknowledgements .....	iv
Dedication .....	v
<b>Chapter 1 Introduction.....</b>	<b>1</b>
Research Objective.....	1
Apoptotic Cell Death in Health and Disease.....	1
The Metastatic Cascade.....	5
<b>Chapter 2 The procoagulant activity of apoptotic cells supports circulating tumor cell survival.....</b>	<b>8</b>
Introduction .....	8
Results .....	9
Discussion .....	21
<b>Chapter 3 Exploring additional mechanisms by which apoptotic cells influence metastasis .....</b>	<b>25</b>
Introduction .....	25
Results .....	27
Discussion .....	30
Closing Remarks and Impact .....	33
Figures.....	35
Materials and Methods.....	47
References.....	54

Portions of this dissertation were adapted from the following publication:

Apoptotic cells promote circulating tumor cell survival and metastasis, Cassidy E. Hagan, Annelise G. Snyder, Mark Headley, Andrew Oberst, bioRxiv 2024.05.21.595217; doi: <https://doi.org/10.1101/2024.05.21.595217>

## List of Figures

### Chapter 1

#### Graphical Abstract

### Chapter 2

**Figure 1.** Circulating apoptotic cells increase lung metastasis in I.V. metastasis models.

**Figure 2.** Effects of apoptotic cells on B16.F10 metastasis in Rag2<sup>-/-</sup> and NK cell depleted animals.

**Figure 3.** Apoptotic cells provide an early survival advantage to tumor cells.

**Figure 4.** Tumor cells undergo apoptosis within 1 hour following I.V. injection.

**Figure 5.** Spatial association of apoptotic cells with tumor cells is necessary for apoptotic cells to exert their pro-metastatic effect.

**Figure 6.** Apoptotic cells promote platelet aggregation on tumor cells and the effect of apoptotic cells on metastasis depends on coagulation.

**Figure 7.** Apoptotic cells have enhanced procoagulant activity.

**Figure 8.** Phosphatidylserine exposure promotes the coagulant activity of apoptotic cells.

**Figure 9.** Tissue Factor is responsible for the magnitude of apoptotic cell enhanced metastasis and platelet clotting in the lung.

### Chapter 3

**Figure 10.** Lung Myeloid Gating Scheme.

**Figure 11.** Metastasis Associated Macrophages are recruited to the lungs and phagocytose apoptotic material.

**Figure 12.** Phagocyte depletion reduces metastasis in Met-1 model but not B16.F10.

**Figure 13.** MerTK blockade reduced metastasis but did not alter phagocytosis of apoptotic cells.

**Figure 14.** Apoptotic cells enhance tumor organoid growth in low serum conditions.

## **List of Abbreviations**

**3T3**- NIH-3T3 fibroblast  
**AC**- Apoptotic Cell  
**acCasp**- activatable caspase  
**AxV**- Annexin V  
**CTC**- Circulating Tumor Cell  
**Dox**- Doxycycline  
**F/T**- Freeze/Thaw  
**GSDME**- gasdermin E  
**I.V.**- Intravenous  
**MAM**- Metastasis Associated Macrophage  
**MEF**- Mouse Embryonic Fibroblast  
**PS**- Phosphatidylserine  
**TC**- Tumor Cell  
**TF**- Tissue factor  
**UV**- Ultraviolet

## **Acknowledgements**

This dissertation research wouldn't be possible without the support of a wide range of individuals who supported my scientific and personal growth throughout my PhD. My thesis advisor, Andrew Oberst, was instrumental in the conceptualization of this project and carefully guided me to create a meaningful story. Andrew always prioritized providing thoughtful and prompt feedback whenever I was writing a grant, preparing for a presentation, or considering important next steps for experiments. His talent in telling compelling scientific stories guided the development of my scientific communication, a skillset that I am enthusiastic to pursue as a future career. I am also immensely thankful to my thesis committee, Jessica Hamerman, Mark Headley, Kevin Urdahl, and Kevin Cheung who helped me hone my project to actionable and feasible goals. Thank you to all members of the Oberst lab, past and present, who listened carefully and always provided thoughtful feedback. Their empathy and support was essential to progressing forward despite various challenges. Through this, these colleagues became family.

Through all the challenges of graduate school, my friends and family always took care of me, making sure I maintained a vibrant and fulfilling life outside of lab. I especially want to thank the following people for their unconditional support. Rachel Van Gelder who listened to every one of my complaints, empathized, and provided me with resources to take care of myself during the hardest challenges. Aaron Ohnsorg who loved and cared for me, making sure I was fed, rested, relaxed and enjoying life no matter what my mood was. My sister, Shannon for always reminding me the importance of family and my parents, Mara and Chris, for helping me make all of my biggest life decisions including encouraging me to pursue graduate school in the first place.

## **Dedication**

This work is dedicated to all of the teachers who fostered my sense of curiosity for the world. Especially those who went above and beyond to make learning fun.

# Chapter 1 Introduction

## Research Objective

For the majority of cancer therapies, elimination of the primary tumor is achieved by directly stimulating the death of cancer cells, predominantly through the programmed cell death pathway apoptosis. However, the presence of apoptotic cells is known to initiate tissue repair programs including promoting cell proliferation, angiogenesis, and dampening immune responses<sup>1</sup>. Clinical correlations between high levels of apoptosis and poor outcomes have been observed in multiple tumor types<sup>2-8</sup>. Experimental evidence to explain these observations include: selection for aggressive cancer clones<sup>9</sup>, release of proliferative signals<sup>10</sup>, and recruiting and reprogramming macrophage populations<sup>11</sup>. These studies characterizing the influence of apoptosis on cancer progression have focused on effects within the primary tumor. Although metastasis is the primary cause of morbidity and mortality in cancer, little is known about the role of apoptotic cell death in modulating metastasis. The overall objective of this dissertation research was to investigate the impacts of apoptotic cells on metastasis and define the specific signals from apoptotic cells which alter the fate of metastatic cells. We hope that this work may inform therapeutic strategies which combat the pro-metastatic effects of apoptotic cell death.

## Apoptotic Cell Death in Health and Disease

Roughly 50 billion cells undergo apoptosis in our bodies each day. Apoptosis occurs during a wide range of physiological processes ranging from tissue development and maintenance to controlling infections. In all of these situations, apoptosis plays an important role in maintaining and restoring homeostatic balance. Perturbations in the proper execution and

responses to apoptotic cell death can lead to a number of disorders such as autoimmunity, cancer, and aberrant inflammation.

Apoptosis plays a critical role in maintaining tissue homeostasis by eliminating unnecessary, defective, aberrantly proliferative, or infected cells<sup>12</sup>. During development, cells communicate with their neighbors, telling each other when to die in order to reveal tissue structure. An example of this is during digitization, the formation of individual fingers. Cells that are present in the interdigital regions undergo apoptosis to form the structure of hands. Apoptosis is also critical in the development of the adaptive immune system, where large quantities of lymphocytes are created; those that do not meet the stringent requirements for reactivity of their antigen receptor are deleted by apoptosis so as not to cause autoimmunity or lymphoma. Apoptosis is also an important cancer prevention strategy. Potentially cancerous mutations in cells occur often, however cells have various checkpoints in place to recognize when DNA damage has occurred or the cell is replicating out of control and eliminate the cell before it can become a danger to the tissue. In its most basic form, apoptosis can also be thought of as an immune effector pathway. Cells that are infected with a pathogen will undergo apoptosis in order to eliminate the replicative niche of the pathogen, thereby preventing spread to other cells.

Indicative of its ubiquitous role as a regulator of cell fate under a variety of circumstances, apoptosis can be triggered through a variety of mechanisms. Cells must integrate numerous signals to determine their fate. Broadly, the induction of apoptosis can be categorized into two main initiation pathways, termed intrinsic and extrinsic apoptosis<sup>13</sup>. Intrinsic apoptosis can occur after a range of intracellular events such as DNA damage, transcriptional abnormalities, and replicative stress. This process is regulated by the balance of pro- and anti-

apoptotic members of the BCL-2 family of proteins<sup>14</sup>. Expression levels of BCL-2 proteins are regulated through a variety of transcriptional pathways allowing cells to integrate a huge amount of information in order to determine the propensity of the cell to die. When the balance of pro-apoptotic BCL-2 proteins outweighs the anti-apoptotic proteins, the effector BCL-2 proteins, Bax and Bak, permeabilize the mitochondrial outer membrane, releasing SMAC and Cytochrome-C into the cytosol. SMAC antagonizes the caspase-9 inhibitor XIAP while Cytochrome-C facilitates oligomerization of APAF-1, ultimately allowing activation of Caspase-9. Extrinsic apoptosis is mediated by activation of death receptors on the cell surface, providing a way for cells to receive direct cues from neighboring cells to undergo cell death<sup>15</sup>. These death receptors include TNFR, TRAILR, and Fas, all containing death domains which activate caspase-8. Activated caspase-8 and caspase-9 are both able to cleave the executioner Caspases 3 and 7 which are responsible for the highly ordered demise of the cell.

Caspases are a family of protease enzymes whose targets define the morphological changes associated with apoptotic cell death<sup>16</sup>. Numerous caspase targets exist, resulting in canonical features of apoptosis such as cell shrinkage, membrane blebbing, externalization of phosphatidylserine (PS) from the inner to the outer leaflet of the plasma membrane, DNA degradation, and chromatin condensation. This highly ordered degradation of the cell is necessary for the subsequent proper clearance of dead cells. To facilitate their clearance, apoptotic cells secrete and display “find-me” and “eat-me” signals that recruit and engage phagocytes<sup>17</sup>. Caspase activation results in the cleavage and opening of PANX1 channels which release intracellular metabolites such as ATP, forming a chemotactic “find-me” gradient for phagocytes<sup>18</sup>. Additionally, caspases are responsible for exposure of PS to the outer membrane, an important indication that a cell is undergoing apoptosis. Caspases expose PS by inactivating

the phospholipid flippase ATP11C, which transports PS to the inner leaflet of the plasma membrane in live cells, and activating the scramblase XKR8, which shuffles the phospholipids between the inner and outer plasma membrane<sup>19,20</sup>. PS is recognized by numerous receptors as an “eat-me” signal, initiating phagocytosis of apoptotic cells. PS receptor ligation results in actin cytoskeleton rearrangement and phagocytosis of the apoptotic cell. PS dependent engulfment of apoptotic cells induces secretion of anti-inflammatory cytokines such as TGF $\beta$  and IL-10 and blocks NF $\kappa$ B-dependent inflammatory signaling to maintain tolerance to apoptotic cells<sup>21</sup>.

Rapid clearance of apoptotic cells by phagocytes is required to prevent detrimental inflammation associated with recognition of cellular debris by other cells. If apoptotic cells are not effectively cleared, they become secondarily lytic, releasing inflammatory molecules and triggering immune responses to intracellular antigens. Secondary lysis is regulated by the pore forming molecule gasdermin E which is cleaved by caspase-3<sup>22</sup>. Inducing apoptosis in tumors with high gasdermin E expression leads to improved anti-tumor adaptive immunity<sup>23</sup>. Defects in phagocytosis of apoptotic cells result in the buildup of secondarily lytic cells and can lead to Systemic Lupus Erythematosus, an autoimmune disease directed against self DNA and DNA associated molecules that are released by lytic cells<sup>24</sup>. Thus, efficient clearance of apoptotic cells is central to maintaining the immunologically silent nature of apoptosis.

Apoptosis is ubiquitous throughout physiological processes and the appropriate response the apoptotic cell death is required to maintain homeostasis. Cancer is a disease where apoptosis is often dysregulated, leading to aberrant cell proliferation. Thus cancer therapies seek to induce apoptosis within tumor cells. However, the primary physiological response to large amounts of apoptotic cells is immunosuppression and tissue-repair programs. It was shown that tumor regrowth after radiotherapy was dependent on caspase-3 which regulates the production of

PGE<sub>2</sub>, a potent growth factor and anti-inflammatory molecule<sup>10</sup>. Additionally, in a model of B cell lymphoma, apoptotic tumor cells lead to the accumulation of macrophages which supported angiogenesis and tumor growth, exemplifying the wound-repair effects of apoptotic cell death<sup>11</sup>.

Together, the well-defined role of apoptotic cells during normal physiology and the initial demonstrations that apoptotic cells have various pro-tumor effects highlights the need to further explore the role of apoptotic cells at all stages of tumor progression. Notably, the effects of apoptotic cells in circulation during metastasis is not yet explored.

### **The Metastatic Cascade**

Metastatic disease, caused by the dissemination of tumor cells from a primary tumor to distant tissues, is the major cause of mortality in cancer patients<sup>25</sup>. The metastatic cascade is a complex multistep process involving coordination between tumor cells, accessory cells, and the microenvironment.

Cancer cells of the primary tumor must acquire the ability to detach from their matrix and enter circulation. Tumor associated macrophages can contribute to this by promoting angiogenesis and providing signals which enhance tumor cell invasion and motility<sup>26</sup>. In an effort to explain the high rates of metastasis in post-partum breast cancer patients, it was determined that apoptosis of mammary epithelial cells during mammary gland involution resulted in macrophage secretion of TGF- $\beta$  which supported metastatic dissemination<sup>27</sup>.

Next, circulating tumor cells (CTCs) must create a supportive niche to allow their survival in the hostile circulatory environment and upon arrest at distant tissue sites. Tumor cells in circulation experience diverse stresses such as shear stress and deformation as they travel through small capillaries. The mechanosensitive pannexin-1 channel releases ATP upon cell deformation which can signal in an autocrine manner to support cell survival<sup>28</sup>. Most CTCs

upon arresting in the lung release membrane blebs that are sampled by myeloid cell populations<sup>29</sup>. Coagulation and platelet activation can also support CTC survival in circulation. Expression of Tissue factor on CTCs causes the accumulation of activated platelets around CTCs<sup>30</sup>. Platelet activation releases survival signals and protect CTCs from shear stress and natural killer (NK) cell recognition<sup>31-37</sup>.

After aggregating on tumor cells platelets release CXCL5 and CXCL7 which recruits neutrophils to the early metastatic niche<sup>38</sup>. Neutrophils have been shown to have pleiotropic roles in metastatic dissemination<sup>26</sup>. In circulation, they typically have been observed to play a pro-metastatic role, supporting CTCs by facilitating tumor arrest, inhibiting NK cells, releasing IL1 $\beta$  and metalloproteinases to support extravasation, and activating cell-cycle progression<sup>39-41</sup>. Recruitment of monocytes to the forming metastatic niche is also dependent on platelet activation by tumor cells<sup>42</sup>. Monocytes and monocyte-derived macrophages facilitate extravasation and growth of metastatic cells<sup>43,44</sup>. Extravasation can also be directly enhanced by platelet derived ATP which signals on endothelial P2Y<sub>2</sub> receptors which increase endothelial permeability<sup>45</sup>.

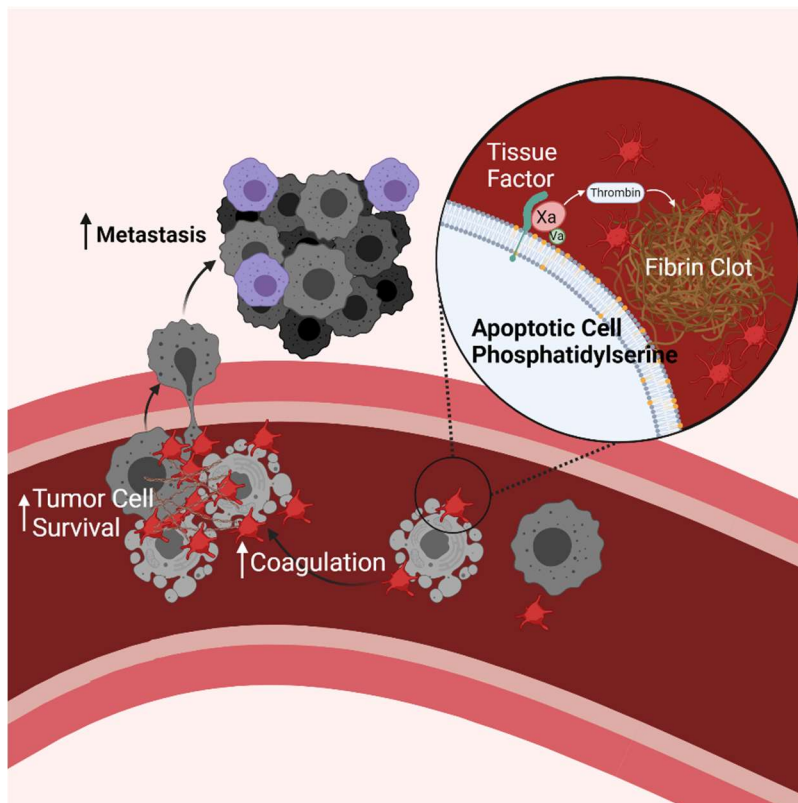
Growth of tumor cells in a novel organ is dependent on a wide variety of factors depending on tumor cell origin and metastatic organ. Often, disseminated tumor cells may lie dormant for long periods before still unknown factors activate their growth<sup>46</sup>. This dormancy and reactivation is particularly problematic for patients with minimum residual disease, where the primary tumor may have been effectively eliminated but a few dormant cancer cells remain in the body, threatening the patient with relapse and metastatic tumor growth.

There are a variety of stages along the metastatic cascade where apoptotic cells could influence metastatic dissemination. Within the tumor microenvironment, apoptosis could

polarize macrophages to support tumor cell intravasation and their epithelial to mesenchymal transition. In circulation, apoptotic cells could engage with a number of immune cells or directly with tumor cells to support tumor cell survival in the harsh circulatory environment. Once at the metastatic site, apoptotic cells could influence macrophages which contribute to CTC extravasation and subsequent outgrowth.

The complexity of both the metastatic cascade and the effects of apoptotic cells poses a challenge to uncovering key effects apoptotic cells might have during metastatic dissemination. In this dissertation research, we aim to home in on the role of apoptotic cells specifically during the intravascular phase of metastatic dissemination. We hope these efforts yield insightful mechanisms into the biology of metastatic dissemination and the potential consequences of apoptotic cell death during cancer progression.

### Graphical Abstract



## Chapter 2 **The procoagulant activity of apoptotic cells supports circulating tumor cell survival**

### **Introduction**

Overall, the metastatic process is extremely inefficient. Experiments tracking the fate of CTCs have found that <1% of cells survive the stresses associated with vascular dissemination<sup>43,47</sup>. Recognition by immune cells as well as shear stress leads to the demise of a majority of CTCs before they can arrest, extravasate and form a metastatic tumor. While most research has focused on characteristics that allow rare CTCs to successfully metastasize, very little is understood about the effects of the greater portion of tumor cells that die during the process of metastasis. Studies examining CTCs have found that a large proportion show molecular features of apoptosis, and in patients with breast cancer, the presence of apoptotic CTCs is correlated with progression to metastatic disease<sup>48-52</sup>. However, experimental evidence evaluating the effect of circulating apoptotic cells on metastasis is lacking.

Ultimately, we show that apoptotic cells in circulation potently enhance metastasis by promoting the survival of CTCs. This effect requires the physical association of apoptotic cells with CTCs at sites of metastatic colonization, and is driven by the promotion of coagulation and platelet aggregation by apoptotic cells. The procoagulant activity of apoptotic cells is dictated by Tissue factor (TF) activation, which occurs upon PS externalization on the apoptotic cell surface. The ability of apoptotic cells to promote metastasis correlates with the colocalization of tumor cells and apoptotic cells within platelet clots, establishing apoptotic cells as an important contributor to the early metastatic microenvironment supporting tumor cell survival in circulation.

## Results

### 2.1 Circulating apoptotic cells increase lung metastasis in I.V. metastasis models.

Given the clinical correlation between apoptotic CTCs and progression to metastasis in patients with breast cancer<sup>48,49</sup>, we sought to design a system in which we could directly assess the impact of circulating apoptotic cells during hematogenous dissemination of breast cancer. To do this, Met-1 cells, a mammary tumor cell line derived from MMTV-PyMT transgenic mice<sup>53</sup>, were injected intravenously (I.V.) into syngeneic (FVBN/J) immunocompetent mice alone or with an equal number of apoptotic cells (**Fig. 1A**). The I.V. metastasis model allows synchronization of key steps after CTC entry into circulation allowing for precise quantification of CTC arrival, survival and fate in the lung vasculature.

Apoptotic cells were prepared from cells lines expressing caspase-8 or caspase-9 fused to activatable FKBP<sup>F36V</sup> dimerization domains (hereafter acCasp8, acCasp9). Incubating these cells with the nontoxic ligand B/B, a synthetic bivalent homolog of rapamycin, enforces caspase dimerization and activation. This system, which we and others have used in the past, gives us precise control over the activation of apoptosis<sup>54-57</sup>. After a short pulse incubation with B/B *ex vivo* cells are committed to undergo apoptosis and are immediately processed for I.V. injections such that apoptotic cells undergo the apoptotic cascade *in vivo*. Inducing apoptosis through acCasp9 resulted in rapid externalization of PS while acCasp8 activation or ultraviolet (UV) irradiation resulted in slower, more heterogeneous apoptotic cell death. In all cases, induction of apoptosis led to 100% cell death as measured by membrane permeability (**Fig. 1B**). Necrotic cells killed by freeze/thaw (F/T) lysis<sup>58</sup>, rather than additional live cells, served as a control for increased total cell number in mice injected with tumor cells + apoptotic cells as a majority of live cells undergo apoptosis *in vivo* following I.V. injection. Fourteen days following I.V.

injection of Met-1 cells alone or Met-1 cells mixed with dying cells, mice were euthanized and the number of metastatic nodules on the lung surface was quantified.

We observed that coinjection of apoptotic Met-1 cells with viable Met-1 cells increased the metastatic burden by approximately three-fold, while necrotic Met-1 cells had no impact on metastasis (**Fig. 1C**). We also examined a model of melanoma metastasis, B16-F10 cells injected I.V. into B6/J mice, and found a similar increase in metastasis with coinjection of apoptotic but not necrotic tumor cells (**Fig. 1D**). Induction of apoptosis in B16-F10 cells through both UV irradiation and acCasp9 activation had similar effects. We confirmed that apoptotic cells themselves could not form metastatic nodules; injecting only apoptotic cells resulted in no detectable tumor foci in the lung (**Fig. 1B-C**).

To examine whether this was a general feature of apoptotic cells regardless of cell type, we tested the effect of coinjecting apoptotic NIH-3T3 fibroblasts (3T3) in Met-1 and B16-F10 metastasis models. Strikingly, apoptotic 3T3s enhanced Met-1 metastasis by approximately 20-fold (**Fig. 1E-F**). Apoptotic 3T3s had a similar effect on B16-F10 metastasis as apoptotic B16-F10 cells (**Fig. 1G**).

We confirmed that the allogenicity of 3T3s was not a relevant variable by observing that autologous mouse embryonic fibroblasts (MEF) stimulated to undergo apoptosis with UV irradiation also enhanced Met-1 and B16-F10 metastasis to a similar degree as apoptotic 3T3s (**Fig. 1H-I**). Our finding that allogeneic and autologous apoptotic fibroblasts as well as apoptotic tumor cells enhance metastasis suggests that the promotion of metastasis is a general feature of apoptotic cells, regardless of their origin.

As observed with necrotic Met-1 and B16-F10, necrotic 3T3 fibroblasts had no effect on metastasis in either model (**Fig. 1F-G**). Inducing necroptosis, a form of programmed lytic cell

death, through acRIPK3 oligomerization in 3T3 cells<sup>54,57</sup> also had no impact on metastasis. The caspase-3 cleavable pore-forming protein gasdermin E (GSDME) is responsible for secondary necrosis following apoptosis<sup>22</sup>. Doxycycline (Dox) controlled overexpression of GSDME, caused cells to progress to secondary necrosis rapidly upon caspase activation, comparable to the rate of lysis after acRIPK3 oligomerization (**Fig. 1J**). However, GSDME expression did not impact the ability of acCasp9 cells to enhance metastasis (**Fig. 1K**). Together this suggests that caspase-independent lytic cell death does not promote metastasis, however, cell lysis following caspase activation does not terminate the pro-metastatic effect of apoptotic cells.

## **2.2 Apoptotic cells provide a survival advantage to circulating tumor cells.**

We next sought to address where, along the metastatic cascade, apoptotic cells exerted their prometastatic effects. We first examined whether apoptosis might act by suppressing adaptive immune surveillance of metastatic cells by examining their effect in *Rag2*<sup>-/-</sup> mice, which lack T and B cells. Apoptotic cells retained their ability to promote metastasis in *Rag2*<sup>-/-</sup> mice, indicating that the adaptive immune compartment was not a primary driver of the effects of apoptotic cells (**Fig. 2A**). Next, to examine the contribution of NK cells which play an important role in restricting CTC survival<sup>59,60</sup>, we administered an NK depletion antibody (anti-NK1.1) 72 and 24 hours prior to I.V. metastasis challenge. Although depleting NK cells resulted in substantially higher metastatic burden, as previously reported<sup>61</sup>, apoptotic cells still provided a metastatic advantage, suggesting that apoptotic cells are acting via a mechanism other than protecting tumor cells from NK cell killing (**Fig. 2B-C**).

We next sought to assess when during the dynamic process of tumor cell arrest, survival and extravasation apoptotic cells exert their pro-metastatic effect. To quantify tumor cell seeding and subsequent survival we used qPCR to measure tumor-specific genomic DNA (PyMT

transgene) in the lung at timepoints from 5 minutes to 96 hours post I.V. injection. Maximum tumor cell quantity in the lung was observed as early as 5 minutes following I.V. injection, indicating rapid arrest of tumor cells in the lung vasculature. This initial seeding was not affected by the co-administration of apoptotic cells. The relative quantity of tumor cells declined exponentially over the next 24 hours as previously reported<sup>43</sup> (**Fig. 3A-B**). We concurrently quantified apoptotic cell genomic DNA in the lung and as expected apoptotic cells showed a similar logarithmic decline in abundance over 24 hours, concomitant with their uptake by CD45+ phagocytes (**Fig. 3 C-E**). We found that tumor cell survival (as measured by persistence of tumor genomic material over the first 24 hours) was increased in the presence of apoptotic cells. Coinjection of Met-1 tumor cells with apoptotic 3T3 cells resulted in an increase in PyMT gDNA (Met-1 cells) of approximately 4-fold at 6 hours post-injection and 50-fold at 24 hours post-injection (**Fig. 3A**). Met-1 cells expressing ZsGreen to distinguish them from coinjected apoptotic acCasp9 Met-1 cells also showed increased gDNA persistence in the lungs at 6 and 24 hours post-injection relative to Met-1 cells injected alone (**Fig. 3B**). We observed similar trends when quantifying tumor cells in the lung by flow cytometry and by fluorescent imaging: apoptotic cells increased the persistence of tumor cells at 6 and 24 hours post-administration (**Fig. 3F-G**). This indicates that both apoptotic fibroblasts and apoptotic tumor cells promote the persistence of live tumor cells over the first 24 hours after arrival in the lung vasculature.

The exponential decline in tumor cell persistence over the first 24 hours after I.V. injection is likely a result of those cells undergoing apoptosis themselves. At one hour post-injection, we examined tumor cells for cleaved caspase-3 (CC3), a marker of active apoptosis, and observed that an average of 70% of tumor cells were positive for CC3 (**Fig. 4A**) and 40-60% of tumor cells externalized PS (**Fig. 4B-C**). This suggests that a vast majority of tumor cells

themselves are undergoing apoptosis. We observed a reduction in the fraction of PS+ tumor cells at 1-hour post-injection when they were coinjected with apoptotic cells (**Fig. 4D**).

Together, these data suggest that apoptotic cells improve CTC survival by protecting tumor cells during this critical window of lung seeding.

We sought to address whether temporal or spatial separation of apoptotic cells from tumor cells affected metastatic burden by injecting apoptotic cells 24 hours prior to tumor cell challenge, or sequentially into the opposite tail vein from tumor cells. Pre-injecting apoptotic cells 24 hours prior had no effect on metastatic burden in the lung, suggesting that apoptotic cells do not have long-lasting effects that impact CTC survival (**Fig. 5A**). Injecting apoptotic cells and tumor cells within one minute of each other, but into separate vascular sites, also abrogated the prometastatic effect of apoptotic cells (**Fig. 5A-B**). These data indicate that apoptotic cells must enter circulation alongside viable tumor cells in order to have a prometastatic effect.

Tumor cells physically associated in clusters with other cells have been shown to have a metastatic advantage over single tumor cells<sup>40,62,63</sup>. Given that the murine lung contains over 1km of total vasculature<sup>64</sup>, we examined whether injecting apoptotic cells and tumor cells in separate veins reduced their physical association within the lung. When injected together, apoptotic cells were often localized in close proximity to tumor cells within the lung (**Fig. 5C**). When injected separately into opposite tail veins we observed a reduced percentage of tumor cells in very close proximity to apoptotic cells and an increased average distance between them (**Fig. 5D-E**). Injecting tumor cells and apoptotic cells in separate tail veins rather than mixed together did not impact the number of tumor or apoptotic cells that seeded the lung. (**Fig. 5F-G**).

Given these findings, we considered the possibility that tumor cells might receive pro-survival signals from apoptotic cells during the co-incubation period prior to injection. However,

we found that the duration of *ex vivo* contact between apoptotic cells and tumor cells did not influence their capacity to enhance metastasis. Combining apoptotic and tumor cells immediately prior to injection or up to 1 hour in advance resulted in comparable enhancement of metastasis by apoptotic cells, suggesting that mixing tumor cells and apoptotic cells does not result in pro-metastatic *ex vivo* cell-cell signaling interactions (**Fig. 5A**).

Together, these findings indicate that apoptotic cells promote tumor cell survival following initial seeding of the lung vasculature, and suggest that close spatial association between tumor cells and apoptotic cells *in vivo* is required for apoptotic cells to exert these effects. The spatial and temporal dynamics of apoptotic cell enhancement of metastasis led us to hypothesize that apoptotic cells were helping to establish an early protective microenvironment around CTCs.

### **2.3 Apoptotic cells promote platelet aggregation on tumor cells.**

Platelets play an essential role in establishing the early metastatic niche and are critical for the survival of tumor cells in circulation<sup>31–33,38</sup>. Considering that apoptotic cells promote metastasis by improving CTC survival and that this effect requires their spatial association with tumor cells, we hypothesized that apoptotic cells within the metastatic niche may promote platelet-tumor cell interactions. We first examined platelet aggregation on tumor cells injected alone, measuring the difference in platelet clots around CC3+ apoptotic tumor cells and CC3- live tumor cells. We found that a higher percentage of CC3+ tumor cells had platelet aggregation surrounding them compared with CC3- tumor cells. The staining for GP1b $\beta$  was also brighter on CC3+ cells (**Fig. 6A**) This suggests that apoptotic cells may be better at promoting platelet aggregation on the cell surface.

We then compared platelet clots in the lung following injection of tumor cells alone or tumor cells mixed with apoptotic cells. We observed the rapid formation of platelet clots in the lungs after I.V. injection and noticed the clots were often associated with tumor cells and apoptotic cells (**Fig. 6B**). In mice that received tumor cells plus apoptotic cells we observed significantly more platelet clots as well as a larger average size of platelet clots at 15 minutes post-injection (**Fig. 6C**). Platelet clots formed rapidly after tumor cell injection and resolved by 24 hours (**Fig. 6C**). Clots that formed around an apoptotic cell were larger than those around a tumor cell, while clots containing both a tumor cell and an apoptotic cell were the largest (**Fig. 6D**). Platelets aggregated around a higher percentage of tumor cells in mice coinjected with apoptotic cells than in mice receiving only tumor cells and apoptotic cells were localized to these clots (**Fig. 6E**). This indicates that apoptotic cells enhance platelet aggregation on tumor cells.

We next sought to address whether coagulation was required for the pro-metastatic effects of apoptotic cells. To do this we treated mice with the anti-coagulant Low Molecular Weight Heparin (LMWH) prior to I.V. injection of tumor cells alone or tumor cells and apoptotic cells. In both Met-1 and B16-F10 metastasis models we observed that treating mice with LMWH reduced the effect of apoptotic cells on metastasis (**Fig. 6F-H**). This suggests that coagulation is essential for apoptotic cells to promote metastasis.

#### **2.4 Apoptotic cells have enhanced procoagulant activity.**

Given our *in vivo* data indicating a role for coagulation in the promotion of metastasis by apoptotic cells, we sought to directly assess the pro-coagulant activity of apoptotic cells *in vitro*. To do this, we developed an assay based on the prothrombin time coagulation test, a test which measures how fast a clot forms within plasma<sup>65</sup>. We quantified how rapidly live or apoptotic cells formed a fibrin clot in citrated, platelet-poor plasma by measuring the change in absorbance

after addition of  $\text{Ca}^{2+}$  (**Fig. 7A**). A lower time to clot formation indicates higher pro-coagulant activity. When Met-1 or 3T3 cells were stimulated to undergo apoptosis, the apoptotic cells were faster at inducing a fibrin clot compared to their live cell counterparts, as evidenced by a lower time to reach  $V_{\max}$  (**Fig. 7B**). Notably, 3T3 cells were overall faster at initiating coagulation compared with Met-1 cells, mirroring the more robust promotion of metastasis observed upon coinjection of apoptotic 3T3 cells as compared to apoptotic Met-1 cells *in vivo*.

Plasma contact with the cell surface protein TF initiates the extrinsic coagulation cascade<sup>66</sup>. High TF expression on tumor cells has been linked with cancer-associated thrombosis and metastatic progression<sup>42,67-69</sup>. We wondered if the difference in coagulation rates of Met-1 vs. 3T3 cells could be due to differential expression of TF. Consistent with this possibility, Met-1 cells exhibited substantially lower expression of TF than 3T3 or B16-F10 cells (**Fig. 7C**). We therefore generated TF knockout 3T3 cells (3T3 TF<sup>-/-</sup>) or TF overexpressing Met-1 cells (Met-1<sup>TF</sup>) to test whether TF was responsible for their procoagulant activity. Indeed, we observed that the rate of fibrin clot formation induced by each cell type correlated with TF expression. Overexpressing TF on Met-1 cells increased their rate of plasma clot formation while ablating TF on 3T3 cells reduced their rate of plasma clot formation (**Fig 7D-E**). Notably, ablation of TF on 3T3 cells abrogated the higher procoagulant activity of apoptotic cells compared to live cells (**Fig 7E**). This indicates that the speed of clot formation by apoptotic cells depends on TF-mediated coagulation cascades.

TF activates coagulation by forming a complex with Factor VIIa, which catalyzes the conversion of Factor X to Factor Xa. However, TF often exists in an inactive state, termed encrypted TF, on resting cells, which prevents efficient catalysis of this reaction<sup>70</sup>. While the exact mechanisms controlling TF decryption remain incompletely defined, various cell

perturbations, including those that induce PS externalization, can reveal full TF procoagulant activity<sup>70</sup>. We thus directly examined TF activity on live vs. apoptotic cells by assaying the rate of Factor Xa generation in the presence of Factor VII and Factor X. TF on live cells was largely unable to generate Factor Xa irrespective of its expression level suggesting that TF is in the encrypted state on live Met-1 and 3T3 cells. Inducing apoptosis significantly increased TF activity on these cells (**Fig 7F-G**). The magnitude of TF activity after induction of apoptosis was dependent on the level of TF expression. Overexpressing TF on acCasp9 Met-1 or knocking it out on acCasp9 3T3 led to a corresponding increase or decrease of TF activity respectively (**Fig 7F-G**). Together, these *in vitro* data suggest that inducing apoptosis leads to TF decryption, resulting in enhanced procoagulant of apoptotic cells.

Interestingly, when we examined the procoagulant activity of necrotic and necroptotic cells, we found that necrotic cells also have robust procoagulant activity (**Fig. 7H**). Necrotic cells also had enhanced TF activity compared to their live cell counterparts, however the activity was lower than that of apoptotic cells (**Fig. 7I**). We also observed increased clots in the lungs of mice injected with necrotic cells (**Fig. 7J**). This aligns with previous research demonstrating that necrotic cell death can lead to TF mediated coagulation which depends on PS exposure<sup>71</sup>.

## **2.5 Phosphatidylserine exposure promotes the coagulant activity of apoptotic cells.**

PS externalization is an important mediator of thrombosis that occurs during platelet activation and endothelial damage and contributes to other pathological thrombotic events. PS externalization has been described as a mechanism for decrypting TF pro-coagulant activity as well as providing a negatively charged surface for assembly of the FXa-Va-prothrombinase coagulation enzyme complex<sup>70,72-74</sup>. PS externalization is also a canonical feature of the apoptotic plasma membrane; we therefore investigated whether the procoagulant activity of

apoptotic cells was PS-dependent. We employed two distinct strategies to target PS. First, to physically block PS exposed on the outer membrane, we treated cells with saturating concentrations of the PS binding protein Annexin V (AxV). We also generated apoptotic cells that do not externalize PS upon caspase activation by deleting the caspase-activated scramblase XKR8 and expressing a caspase-resistant version of the flippase ATP11c<sup>20</sup> (acCasp9 3T3 Flip<sup>mut</sup>) (**Fig. 8A**). Blocking PS with AxV completely abrogated the ability of TF to generate Factor Xa in the presence of Factor VII and Factor X (**Fig. 8B**). acCasp9 3T3 Flip<sup>mut</sup> cells unable to externalize PS also lacked TF activity after induction of apoptosis. (**Fig. 8B**) These data suggest that TF decryption is dependent on PS externalization during apoptosis.

To examine whether the full procoagulant activity of apoptotic cells was dependent on PS externalization, we next tested these PS blocking strategies in the plasma clot assay. AxV treatment significantly reduced the plasma coagulation rate, however, apoptotic cells treated with AxV still induced clotting faster than live cells treated with AxV (**Fig. 8C**). acCasp9 3T3 Flip<sup>mut</sup> cells also retained an increased plasma coagulation rate upon caspase activation, despite having reduced overall procoagulant activity compared to parental cells (**Fig 8D**). Together this indicates that while TF decryption and maximal procoagulant activity on apoptotic cells is dependent on PS, apoptotic cells have residual, PS-independent procoagulant activity.

We next tested whether blocking PS resulted in reduced metastasis *in vivo*. We found that treatment of apoptotic cells with AxV significantly reduced their ability to promote metastasis (**Fig. 8E**). The early benefit of apoptotic cells on tumor cell survival at 6 and 24 hours was also reduced by treating cells with AxV (**Fig. 8F-G**). This suggests that PS externalization on apoptotic cells benefits early CTC survival and metastasis.

## **2.6 TF expression is required for apoptotic cells to promote clotting *in vivo* and enhance metastasis.**

Given the differential expression levels of TF on Met-1 vs. 3T3 cells (**Fig. 7C**) and the corresponding difference in magnitude of their effect on coagulation and metastasis (**Fig. 1 and Fig. 7B**), we next sought to directly assess the role of TF in the promotion of metastasis by apoptotic cells. TF overexpression on apoptotic Met-1 cells increased their effect on metastasis, to a level comparable to apoptotic 3T3 (**Fig 9A-B**). Conversely, TF knockout reduced the effect of apoptotic 3T3s to a level comparable to that observed with apoptotic Met-1 (**Fig 9C-D**). This suggests that TF expression and the procoagulant activity of apoptotic cells determines the magnitude of effect apoptotic cells have on promoting metastasis.

Given our previous observation that apoptotic cells promoted platelet aggregation at metastatic sites (**Fig 3**), we next assessed the role of TF on apoptotic cells in this process. We found that the lungs of mice coinjected with TF expressing apoptotic cells contained large platelet clots (**Fig 9E**). The intensity of platelet staining associated with apoptotic Met-1 cells overexpressing TF was significantly higher than that observed on unmanipulated Met-1 tumor cells (**Fig 9F**). Increasing TF expression on apoptotic cells significantly increased the number and size of clots found in the lung (**Fig 9G-H**). This suggests that expression of TF on apoptotic cells drives robust platelet activation during vascular dissemination. The relative tumor cell survival at 24 hours was also dependent on TF expression by apoptotic cells. However, TF expression had no impact on tumor cell seeding quantity (**Fig. 9I-J**). This indicates that manipulating the ability of apoptotic cells to form emboli does not simply increase tumor lodgment in the lung, but rather tumor-apoptotic emboli promote tumor cell survival.

Finally, we assessed the role of TF-overexpressing apoptotic cells in promoting aggregation of platelets directly on Met-1 tumor cells with low TF expression. To do this, we quantified the percent of tumor cells within platelet clots and enumerated clots that contained only a tumor cell and those that contained both a tumor cell and an apoptotic cell. Compared to the small increase in tumor cell localization to clots when coinjected with TF-low apoptotic cells, TF-high apoptotic cells led to a substantial increase in the percent of Met-1 tumor cells found within clots. This increase was reflected in the portion of tumor cells localized to a clot that also contained a TF-expressing apoptotic cell, suggesting that TF expression on apoptotic cells can act *in trans* to promote platelet aggregation on tumor cells that have low TF expression. (**Fig. 9K**)

We also examined whether injecting apoptotic cells separately from tumor cells, into opposite tail veins, had an effect on the localization of tumor cells and apoptotic cells within clots. While the overall size and number of clots was not affected by injecting apoptotic cells and tumor cells separately (**Fig. 9G-H**), the frequency of tumor cells localized to a clot with an apoptotic cell was decreased (**Fig. 9K**). This indicates that when apoptotic cells and tumor cells are injected separately, they are less likely to localize together within clots. Because injecting tumor cells and apoptotic cells in separate veins reduces their effect on metastasis (**Fig. 5A-B**) and the effects of apoptotic cells are dependent on their ability to trigger coagulation through TF (**Fig. 7,9**), we postulate that tumor cells localized together in a clot with an apoptotic cell are more likely to survive and form a metastatic nodule. Together, these findings identify a previously unappreciated role for apoptotic cells in promoting metastasis, and suggest that TF expression by apoptotic tumor cells is a key contributor to this process.

## Discussion

Killing tumor cells by apoptosis is a central goal of most tumor therapies. Counterintuitively however, an expanding body of evidence suggests that the presence of apoptotic cells, from either tumor or stromal origin, may correlate with increased tumor growth and negative clinical outcome. While apoptotic cell death within tumors is known to promote tumor cell proliferation, angiogenesis, and pro-tumor macrophage polarization<sup>1,8,75</sup>, a putative role of apoptotic cells throughout the metastatic cascade has not been well defined. Here we report a striking role for apoptotic cells in facilitating metastasis by supporting early CTC survival. We find that the effect of apoptotic cells on metastasis depends on the pro-coagulant activity of TF, which is induced upon PS exposure on apoptotic membranes.

In imaging the early seeding of CTCs in the lungs, we observed that apoptotic cells promote platelet aggregation, and that the colocalization of apoptotic cells with tumor cells thereby supported CTC survival. Platelet aggregation on tumor cells is important for shielding tumor cells from NK cell cytotoxicity and reducing shear stress, two significant contributors to early CTC demise<sup>31-36</sup>; our findings suggest that the presence of apoptotic cells offers a mechanism for CTCs to activate coagulation to survive these pressures. Extrinsic coagulation mediated by TF is rapid, and intravascular aggregation of CTCs is rare<sup>63</sup>; thus, when apoptotic and tumor cells do not enter circulation together—modeled herein as separate injections into opposing tail veins—apoptotic cell-induced coagulation would not occur in proximity to a tumor cell, thus abrogating the metastatic benefit conferred by apoptotic cells. It has been observed that CTC clusters have significantly enhanced metastatic potential when compared to individual CTCs<sup>62,63,76,77</sup>. CTC clusters disseminate collectively, entering circulation as a single unit<sup>62,63</sup>, and thus represent a physiological context in which an apoptotic cell could be localized with a

tumor cell in circulation. While, various pro-metastatic characteristics of CTC clusters have been defined such as stemness, apoptosis resistance, and immune escape <sup>76,77</sup>, the presence of apoptotic cells within clusters has not been investigated. An intriguing possibility for one metastatic advantage conferred by CTC clusters is that a portion of cells in clusters could undergo apoptosis, thus supporting the survival of other cells within the cluster.

Mechanistically, we find that apoptotic cells initiate robust coagulation through PS mediated TF decryption. An important role of TF expression on CTCs that successfully metastasize has been extensively described <sup>68,78</sup>; however, our work suggests that TF mediated coagulation can also act *in trans* to support CTC survival. Thus, tumor cells with low TF expression, such as Met-1 cells, may depend on apoptosis of other cells as a source of TF activity to facilitate coagulation during vascular dissemination. Fibroblasts have been observed in association with CTCs <sup>79-81</sup> and are a potential source of TF mediated coagulation during metastasis that may be particularly relevant for the survival of TF-low tumor cells in circulation.

Our findings bolster the concept that apoptotic cells are an important procoagulant mechanism in various health and disease settings <sup>82</sup>. TF activity regulated through PS exposure has been described in other disease contexts such as endotoxemia <sup>71,83,84</sup> and vessel injury<sup>85,86</sup>. Most relevant to our model is the consideration of apoptotic cells as a contributing factor to cancer-associated thrombosis <sup>87-90</sup>. Interestingly, the risk of venous thromboembolism increases following chemotherapy <sup>91-93</sup>, a regimen that causes massive apoptosis throughout the body. While chemotherapy has numerous effects beyond induction of apoptosis, our data clearly demonstrate that direct activation of caspases in both tumor and non-tumor cells is a source of procoagulant activity, suggesting that apoptotic cells may be an important contributor to hypercoagulation following chemotherapy.

While our work establishes apoptotic cells as a source of TF and PS-induced coagulation that supports CTC survival in the vasculature, other sources of TF and PS exist and the differential effects of these unique activators of coagulation throughout the metastatic cascade remains an open question. Extracellular vesicles are a source of procoagulant activity and can exhibit pro-metastatic properties<sup>90,94,95</sup>. Apoptosis results in membrane blebbing and release of extracellular apoptotic vesicles, but whether there are distinct outcomes depending on whether EVs are derived from live or apoptotic cells is not clear. Tumor cells themselves have elevated surface PS and targeting PS as a therapeutic strategy has been promising<sup>21,96-101</sup>. We observed PS externalization on tumor cells in circulation, and interpreted this observation as an early marker of apoptosis. However, it is also possible that deformation and shear stress in circulation results in Ca<sup>2+</sup> flux which could activate the TMEM family of PS scramblases<sup>102</sup>, resulting in PS externalization on live cells. Technical limitations in visualizing externalized PS *in vivo* prevent observation of PS externalization in combination with platelet aggregation, so we cannot yet delineate the potential contributions of PS exposure on live cells to coagulation *in vivo*. Necrotic cells also have procoagulant activity<sup>71,103-105</sup>, yet these cells do not promote metastasis.

Although the procoagulant activity of apoptotic cells is required, additional features of apoptotic cells could be responsible for the differential effect of apoptotic and necrotic cells on metastasis. We do not think that necrotic cells are having a proinflammatory effect, because GSDME overexpression, which induces inflammation in tumors<sup>23</sup>, did not abrogate the prometastatic effects of caspase activation. While numerous possible sources of procoagulant activity exist during metastasis, elucidating the differential subsequent effects of apoptotic cells compared to other sources of coagulation throughout the metastatic cascade is warranted.

While our data highlight the key role of apoptotic cells in initiating coagulation to support metastasis, we are intrigued by the possibility that additional mechanisms exist by which apoptotic cells influence the metastatic process. Apoptotic cells alter their surrounding microenvironment in profound ways. Molecules such as fractalkine, lactotransferrin, and prostaglandin E<sub>2</sub> are released by apoptotic cells to recruit macrophages and can also act on tumor cells to promote survival and proliferation<sup>8,106-109</sup>. Upon caspase activation, apoptotic cells release various anti-inflammatory metabolites from pannexin-1 channels<sup>110</sup>. Interestingly, ATP released through pannexin-1 was demonstrated to have pro-survival signaling in an autocrine manner on CTCs<sup>28</sup>. In the context of a CTC cluster, these various signaling molecules released from apoptotic cells could act in a paracrine fashion to support nearby tumor cells. Furthermore, the interactions between apoptotic cells and macrophages has been extensively characterized as leading to tissue-repair macrophage phenotypes<sup>111</sup>. Previous work has demonstrated that efferocytosis of apoptotic cells within tumors can polarize macrophages, which produce TGF- $\beta$  and other wound-healing cytokines to facilitate metastatic dissemination<sup>112</sup>. CTCs release microparticles upon early arrival in the lung vasculature that are sampled by myeloid cells and guide their differentiation<sup>29</sup>. We observe rapid uptake of apoptotic cells by phagocytes in the lungs; however, whether the interaction between apoptotic cells and phagocytes contributes to the differentiation of metastasis associated macrophages is an open question. The downstream effects of apoptotic cells beyond their most proximal role in inducing coagulation during hematogenous dissemination is an interesting area for future investigation.

## Chapter 3 Exploring additional mechanisms by which apoptotic cells influence metastasis

### Introduction

In Chapter 2, we determine that PS exposure on apoptotic cells which express TF is necessary for apoptotic cells to promote tumor cell survival in circulation and subsequently metastasis formation. Whether apoptotic cells exert additional pro-metastatic effects in addition to ability to promote coagulation during the initial arrest of tumor cells was another question we sought to address. Apoptotic cells can have profound impacts on their environment directly through the release of signaling molecules as well as indirectly through the polarization of phagocytes which clear apoptotic cells. A number of studies have examined the effects of apoptotic cells on cancer progression, finding that apoptotic cells can promote cancer cell proliferation, recruit and polarize tumor supportive macrophages, and dampen anti-tumor immune responses. However, these various pro-tumor impacts of apoptotic cells have not yet been examined in the context of metastatic dissemination. Therefore, we wanted sought to address whether apoptotic cells contribute to metastatic dissemination in additional ways beyond inducing coagulation.

Rapid clearance of apoptotic cells by phagocytes is required to prevent detrimental inflammation associated with recognition of cellular debris by other cells. Macrophages are the primary cell type responsible for clearing apoptotic cells. Upon interaction with apoptotic cells, macrophages acquire anti-inflammatory, tissue-repair phenotypes. In the context of a tumor, macrophages with these phenotypes support tumors by promoting angiogenesis and providing signals which enhance tumor cell growth, invasion and motility<sup>26</sup>. During vascular dissemination, CTCs recruit a population of monocyte-derived macrophages which have been

shown to promote extravasation and growth of metastatic cells<sup>43</sup>. Thus we wondered whether macrophage efferocytosis of apoptotic cells might contribute to metastasis.

Macrophages recognize apoptotic cells through PS receptors. PS receptor ligation results in actin cytoskeleton rearrangement and phagocytosis of the apoptotic cell. PS dependent engulfment of apoptotic cells induces secretion of anti-inflammatory cytokines such as TGF $\beta$  and IL-10 and blocks NF $\kappa$ B-dependent inflammatory signaling to maintain tolerance to apoptotic cells<sup>21</sup>. A number of studies have implicated PS receptor activity in tumor progression and suggested inhibition of this pathway as a therapeutic strategy<sup>21</sup>. Interestingly, a study seeking to understand the mechanisms behind high metastasis rates in breast cancers occurring 2-5 years post-partum found that phagocytosis of apoptotic epithelial cells during mammary gland involution promoted metastatic breast cancer to the lungs<sup>112</sup>. This study showed that inhibiting the PS receptor MERTK prevented metastasis associated with breast involution. Together this suggests that macrophage interactions with apoptotic cells via PS could influence the metastatic cascade.

Apoptotic cells release various signaling molecules into their microenvironment which can have impacts on the proliferation of surrounding cells. In the context of tissue damage, proliferation signals from apoptotic cells are required for proper repair of the tissue<sup>113</sup>. Caspase activity results in the cleavage of the enzyme iPLA<sub>2</sub> which generates arachidonic acid, subsequently converted into other prostaglandins such as PGE<sub>2</sub><sup>114</sup>. PGE<sub>2</sub> has been shown to stimulate tumor growth in multiple tumor models<sup>10,108,115</sup>. We have shown that spatial association between apoptotic cells and tumor cells contributes to the prometastatic effects of apoptotic cells. Therefore, we also addressed whether apoptotic cells might provide survival or proliferation signals in the early metastatic niche.

## Results

### 3.1 Macrophages engulf apoptotic cells and contribute to metastasis

We first examined the recruitment of various myeloid cell populations to the lungs following I.V. injection of tumor cells or tumor cells mixed with apoptotic cells. Using conventional flow cytometry, we identified various subsets of myeloid cells (**Fig. 10**). The various myeloid populations were displayed in a UMAP space for easy visualization of all myeloid cell populations (**Fig. 11A**). We observed, as previously reported for B6/J mice with B16-F10 metastasis, the recruitment of a population of macrophages that are CD11c<sup>+</sup> and MHCII<sup>+</sup> 24 hours after tumor cell seeding of the lungs (**Fig. 11B**). This population is termed metastasis associated macrophages (MAMs) as they are only present following arrival of metastatic cells in the lungs. ZsGreen was expressed in apoptotic cells, allowing us to examine which cells had phagocytosed apoptotic cell derived material. We noted that at 24 hours, patrolling monocytes and MAMs were the primary cell types that contained apoptotic cell material (**Fig. 11C**).

As is apparent from the UMAP plot, mice coinjected with Met-1+apoptotic cells had a large increase in the number of MAM in the lung at 24 hours (**Fig.11B**). However, in a series of repeats using different total cell numbers, we found that the increased MAM population with apoptotic cells was not always reproducible (**Fig. 11D**). Upon examining the variables across experiments, we noted that when we injected a higher number of cells ( $5 \times 10^5$  Met-1 tumor cells) we observed differences in MAM numbers between Met-1 only and Met-1 +Apoptotic cell. In experiments with lower total cell numbers this phenotype was not present. This suggests that there is a threshold of injected cells which leads to increased recruitment of MAM to the lungs. We noted that regardless of whether we observed a difference in MAM population size, we

consistently observed a significant increase in tumor cell survival with apoptotic cell co-administration (**Fig. 11D**). This suggests that a difference in the number of recruited MAMs does not drive the early survival advantage of tumor cells coinjected with apoptotic cells.

An alternative hypothesis by which apoptotic cells promote tumor cell survival and metastasis is by overwhelming the phagocytic capacity *in vivo* thereby leaving tumor cells un-engulfed. To examine this possibility we measured engulfment of ZsGreen<sup>+</sup> tumor cells by CD45<sup>+</sup> phagocytes with and without apoptotic cells. We observed a decrease in the frequency of un-engulfed tumor cells (CD45<sup>-</sup> ZsGreen<sup>+</sup>) and a concomitant increase in engulfed tumor cells (CD45<sup>+</sup> ZsGreen<sup>+</sup>) at 24 hours in mice that received apoptotic cells suggesting that rather than overwhelming phagocytes, the presence of apoptotic cells may enhance phagocytic uptake of tumor derived material. (**Fig. 11E**)

We then sought to address whether phagocytes play a role in the promotion of metastasis by apoptotic cells by depleting phagocytes with clodronate liposomes administered I.V. This approach effectively deletes circulating phagocytic populations. We confirmed depletion of different myeloid cell subsets in the lungs using flow cytometry. Clodronate liposomes reduced the frequency of patrolling monocytes, MAMs, and alveolar macrophages (**Fig. 12A**). The most striking reduction in the myeloid compartment was to CD11c high cells which was also the primary phagocytic population that contained apoptotic cells derived material 24 hours after I.V. injection (**Fig. 12A-B**).

We found that depleting phagocytes in the Met-1 model resulted in a substantial decrease in the effect of apoptotic cells on metastasis (**Fig. 12C**). This suggests that macrophages play a metastasis supportive role as previously described<sup>43</sup> and further rules out the possibility that apoptotic cells are overwhelming the *in vivo* phagocytic capacity. In contrast, depleting

macrophages using clodronate liposomes in the B16-F10 model did not abrogate the effect of apoptotic cells on metastasis, suggesting that macrophages may have unique contributions to metastasis depending on the tumor cell type (**Fig. 12D**). When examining the impact of macrophage depletion on early Met-1 survival with or without apoptotic cells we noted that clodronate treatment did not abrogate the survival advantage of tumor cells coinjected with apoptotic cells at 6 hours, suggesting that the earliest effects of apoptotic cells may not be dependent on macrophages (**Fig. 12E**). We did observe a reduction in tumor cell survival at 24 hours, which supports previous findings that macrophage depletion reduces tumor cell survival at 24 hours (**Fig. 12F**). Together these results indicate that while macrophages support Met-1 metastasis as reported in the literature, they do not seem to be a uniting mechanism required for the effect of apoptotic cells on metastasis in both B16-F10 and Met-1 models.

MerTK is a phagocytic receptor on macrophages which recognizes PS on apoptotic cells and has been implicated in tumor progression<sup>27,116,117</sup>. We examined whether altering uptake of apoptotic cells using a MerTK blocking antibody would have any impact on the effect of apoptotic cells on metastasis. When we examined the uptake of apoptotic material by phagocytes, we noted that MerTK blockade didn't appear to have any impact on the uptake of apoptotic material by any phagocytic population (**Fig. 13A**). Notably, MerTK blockade didn't have any appreciable impact on the uptake of apoptotic material by MAMs. This is likely because MAMs are differentiated from conventional monocytes which do not express high levels of MerTK and are thus likely phagocytosing apoptotic material through another phagocytic receptor. Interestingly, we did observe that blocking MerTK reduced the effect of apoptotic cells on metastasis (**Fig. 13B**). Given that apoptotic cell uptake was not impacted by MerTK blockade however, we hypothesize that MerTK blockade may have been reducing metastasis by a

mechanism not necessarily dependent on the apoptotic cells administered with tumor cells. It is possible that MerTK blockade could have been initiating an interferon response as previously reported<sup>117</sup>.

### **3.2 Apoptotic cells promote proliferation of tumor cells under low-growth factor conditions**

We hypothesized that apoptotic cells may also release factors that could support tumor cell growth. To test this, we measured the effect of apoptotic cells on the growth of tumor organoids cultured in the presence of high, low, or no supplemented growth factors. We found that in the presence of full serum supplementation media, tumor organoids grew rapidly and adding increasing numbers of apoptotic cells provided no growth advantage. Under serum-free conditions, tumor organoids did not form. Interestingly, the presence of apoptotic cells allowed for the survival and growth of tumor organoids in serum-free conditions. There was a dose dependent increase in organoid growth with increasing ratios of apoptotic cells (**Fig 14**). We saw similar results under 1% FBS supplementation. This finding supports findings in the literature that apoptotic cells release survival and proliferation signals which support tumor growth. Whether this mechanism is at play *in vivo* during the early seeding of tumor cells to the lung would be an interesting future question to address. Our data in Chapter 2 suggests that colocalization of tumor cells in a clots with apoptotic cells is required for apoptotic cells to exert their metastasis supportive role. We hypothesize that tumor cells colocalized with apoptotic cells are more likely to survive due to survival and growth factors released from apoptotic cells, as observed in our tumor organoid growth assay.

## **Discussion**

In Chapter 2 we conclude that a significant mechanism driving the enhancement of metastasis by apoptotic cells is their ability to initiate coagulation through PS exposure

enhancing TF activity. An important observation made was that apoptotic cells must colocalize with tumor cells in order for this effect to take place. While this observation may be explained by the fact that platelet aggregation promotes CTC survival and extravasation, we are interested in the possibility that other mechanisms are also at play in this microenvironment.

We show that various monocytes and macrophages phagocytose apoptotic cell derived material, thus it is possible that MAM phenotype and function may be influenced by the presence of apoptotic cells. Especially in the Met-1 model, where macrophages are known to play an important role, we observe that macrophages are required for the effect of apoptotic cells on metastasis. However, it is difficult to parse with the models we used whether they are promoting metastasis specifically through their interaction with apoptotic cells. The contributions of apoptotic cell polarized macrophages on metastatic dissemination is still an open question. Further analysis of macrophage polarization using unbiased analysis such as RNA-sequencing would be an interesting future direction. Additionally, identifying the receptors required for uptake of apoptotic cells by conventional monocytes would allow us to specifically block uptake of apoptotic cells by the precursor population of MAMs. This would be an interesting way to examine whether uptake of apoptotic cells by MAMs contributes to their promotion of metastasis.

We also observe that apoptotic cells are indeed able to support tumor cell survival and growth *in vitro* under low growth factor conditions. A variety of molecules could be responsible for this effect, notably PGE2 has been shown to be released by apoptotic cells and promote tumor growth in primary tumors. PGE2 is rapidly degraded thus this could explain the apparent need for colocalization of apoptotic cells with tumor cells for their impact on metastasis. ATP and other nucleotides are also released during apoptosis as an “eat-me” signal. ATP and UDP

have both been shown to have pro-metastatic effects<sup>28,118</sup>. Whether PGE2, nucleotides or other apoptotic cell derived signaling molecules are acting in a paracrine fashion to promote tumor cell growth and survival would be another interesting question to address. The role of apoptotic cell derived PGE2 could be examined by deleting or mutating the caspase-3 cleavage site on iPLA<sub>2</sub>, the enzyme upstream in the generation of PGE2. Nucleotides are released from apoptotic cells through PANX1 channels, so their role could be examined by deleting or mutating the caspase cleavage site as with iPLA<sub>2</sub>.

Whether the effect of apoptotic cells ends with their role in promoting coagulation or whether there are downstream effects of apoptosis following the initiation of coagulation remains an open question. We are very intrigued by the possibility that apoptotic cells first engage coagulation, which sets up a protective niche for tumor cells and further signals from apoptotic cells contribute to the formation of metastasis by disseminated tumor cells.

## Closing Remarks and Impact

Decades of work has been aimed at finding mechanisms to kill tumor cells, primarily through inducing apoptosis. Our work supports a growing body of evidence that apoptosis in the context of cancer can have adverse pro-tumor effects. Eliminating tumor cells, primarily through apoptotic cell death, will remain the primary goal of cancer therapeutics. However, understanding the subsequent effects of apoptosis on cancer progression could inform additional interventions countering the pro-tumor secondary effects of apoptosis. For example, blocking apoptosis by inhibiting caspase activation results in the conversion of apoptosis to an inflammatory form of cell death capable of enhancing anti-tumor immunity<sup>119</sup>. Whether this strategy could also reduce metastasis should be addressed. Because we define apoptotic cells as an important source of coagulation and show that LMWH treatment reduces the effect of apoptotic cells in promoting metastasis, targeted anti-coagulants are another possible therapeutic strategy. Temporal administration of anti-coagulants or the use of PS or TF blocking agents during times where high levels of apoptosis are expected, such as during cytotoxic therapy, could specifically target coagulation initiated by apoptotic cells. While the use of anti-coagulants has been proposed as a potential therapeutic to reduce metastatic spread<sup>120,121</sup>, they are not yet broadly used as anti-metastatic agents. The safety and efficacy of anti-coagulants in patients at risk for cancer-associated thrombosis is being evaluated<sup>122,123</sup>; our data suggest that an interesting additional parameter to monitor in these trials could be progression to metastatic disease.

Building upon clinical and experimental evidence that apoptosis can have unintended pro-tumor consequences, this work demonstrates a direct mechanism by which the presence of apoptotic cells during vascular CTC dissemination promotes metastatic disease. By activating

coagulation through PS-dependent TF decryption, apoptotic cells support the survival of tumor cells in circulation. These findings emphasize that it is important to consider not only the cells that directly form metastatic tumors, but also the effects of cells that die throughout the metastatic cascade, opening up new avenues for investigation into the process of metastasis and possibilities for therapeutic intervention.

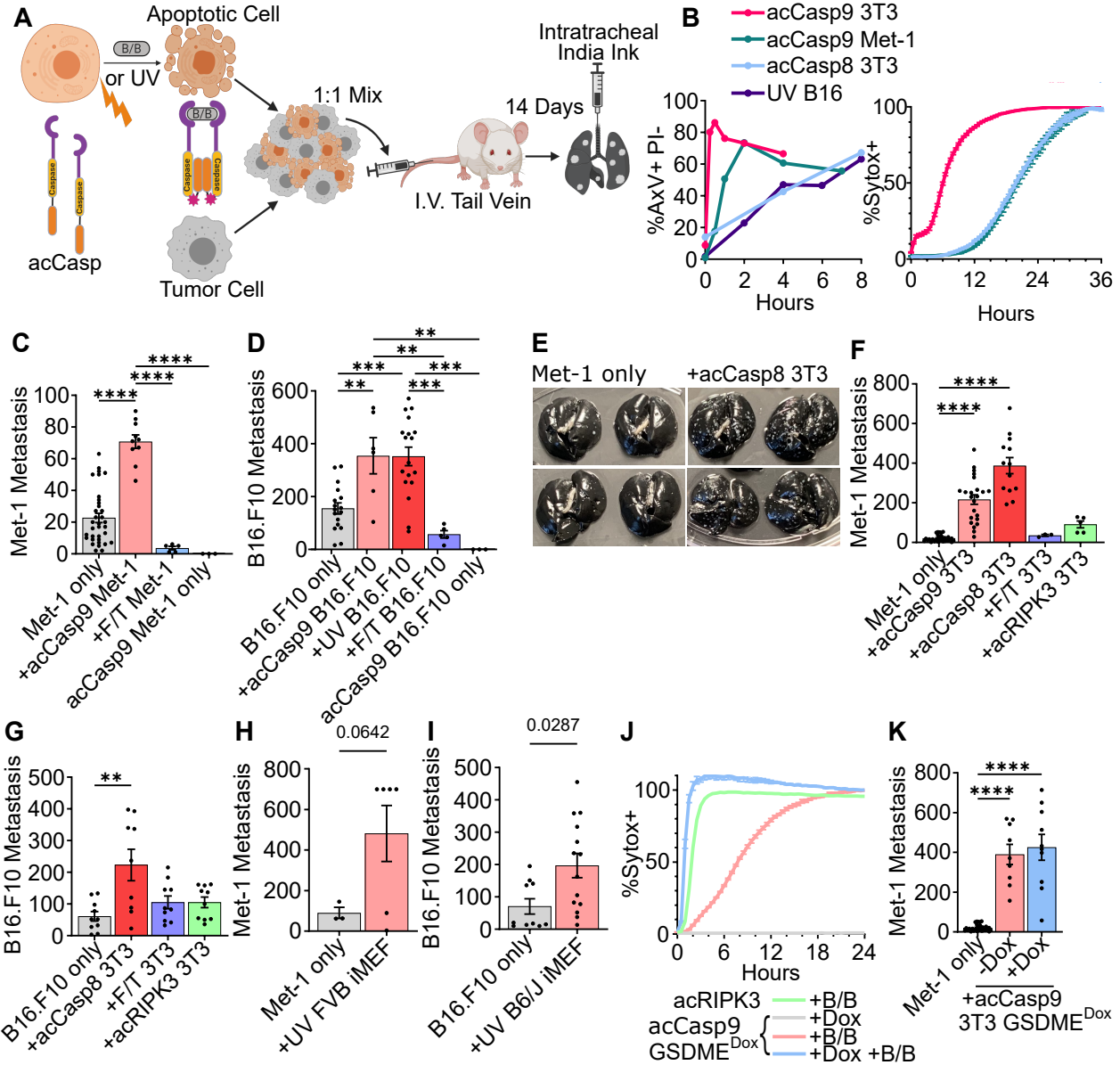


**Figure 1. Circulating apoptotic cells increase lung metastasis in I.V. metastasis models.** acCasp8, acCasp9, or acRIPK3 expressing cells were activated by treatment with B/B for 15 minutes, UV irradiated, or killed by Freeze/Thaw lysis (F/T). PS externalization and membrane integrity on cells after B/B or UV exposure was measured with Annexin V (AxV) and propidium iodide (PI) by flow cytometry (A) or Sytox green with Incucyte live cell imaging. Dying cells were mixed 1:1 with tumor cells and injected I.V., 14 days later surface lung metastasis was quantified (A-I, K). MEFs were derived from FVB/NJ (H) or B6/J (I) mice and immortalized with SV40LT transduction (iMEF). GSDME expression in acCasp9 3T3 GSDME<sup>Dox</sup> cells was induced by doxycycline treatment (+Dox), followed by treatment with B/B to activate acCasp9 (G-H). Membrane permeability was measured by Sytox Green uptake (G). Lungs containing >700 surface metastasis were unable to be accurately quantified due to significant overlap of nodules, thus the maximum value of 700 was recorded in these cases. Dots are biological replicates, Error bars represent SEM, statistical testing is Ordinary one-way ANOVA with Tukey's multiple comparisons test.

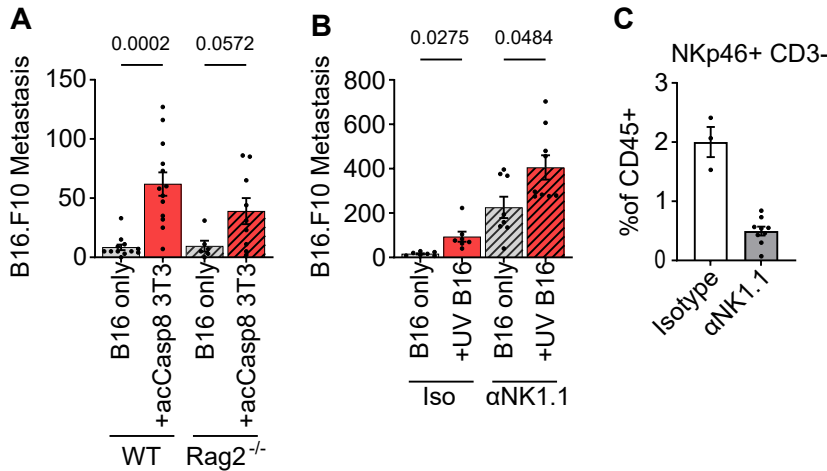


**Figure 2. Effects of apoptotic cells on B16.F10 metastasis in Rag2<sup>-/-</sup> and NK cell depleted animals.** Apoptotic cells were injected at a 1:1 ratio with B16.F10 tumor cells. Surface lung nodules were quantified 14 days after I.V. injection (A-B). NK cell frequency of total CD45<sup>+</sup> cells in the blood was measured 24 hours after I.V. injection of tumor cells to confirm NK cell depletion (C). Dots are biological replicates analyzed by ordinary one-way ANOVA with Tukey's multiple comparisons test.

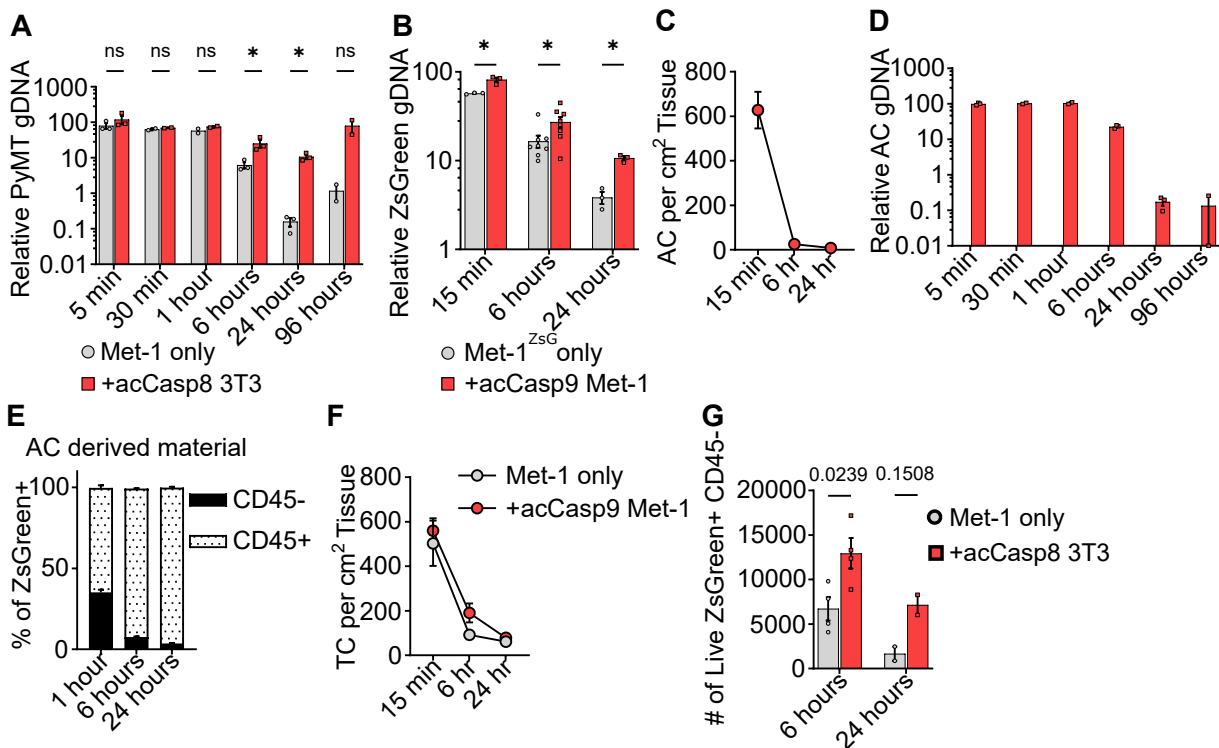


**Figure 3. Apoptotic cells provide an early survival advantage to tumor cells.** Met-1 cells were injected I.V. with acCasp8 3T3 (A, D, E, G) or acCasp9 Met-1 (B, C, F) and lung gDNA was harvested at indicated timepoints for qPCR (A-B, D), fluorescent microscopy (C,F), or flow cytometry (E,G). Tumor cells expressed ZsGreen (B,C,F,G) and apoptotic cells expressed mCherry (C,F,G) or ZsGreen (D,E). Error bars represent SEM, Dots are biological replicates, statistical testing is unpaired t-test. AC=Apoptotic Cell, TC=Tumor Cell

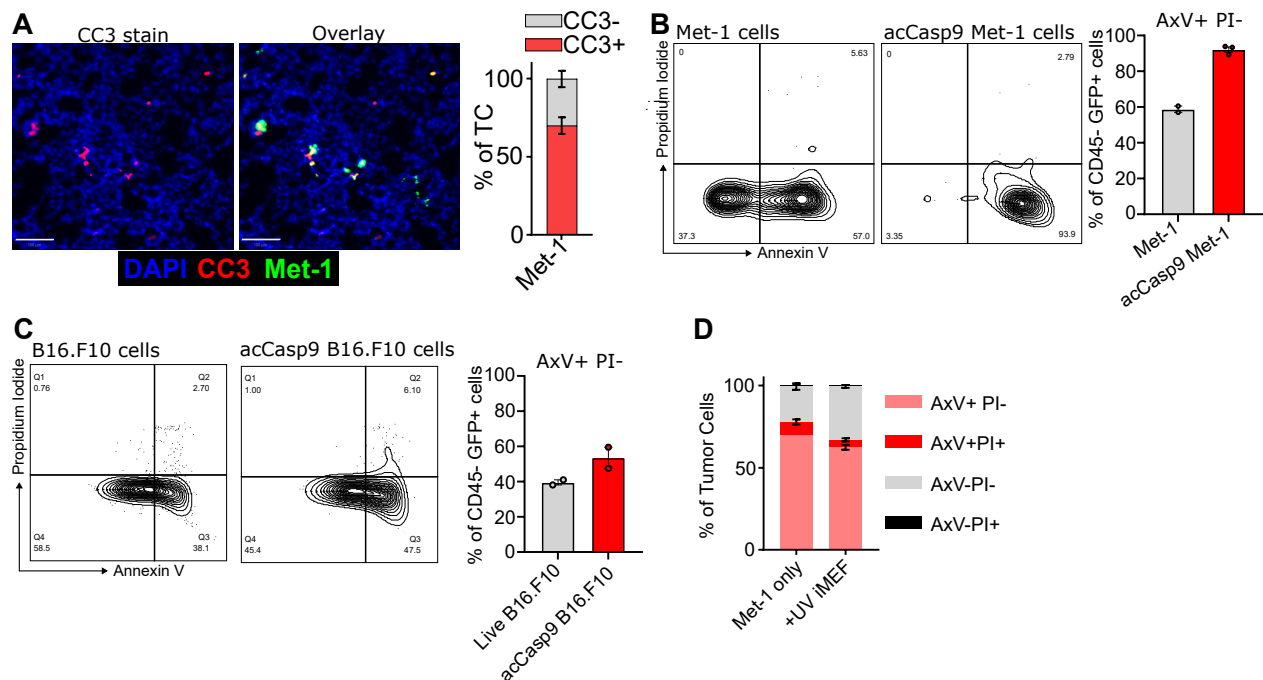


**Figure 4. Tumor cells undergo apoptosis within 1 hour following I.V. injection.** Viable Met-1 (A,B,D) or B16.F10 (C) cells were injected I.V. into mice and lungs were harvested after 1 hour. acCasp9 Met-1 or acCasp9 B16.F10 were activated with B/B for 15 minutes prior to I.V. injection and served as a positive control for PS externalization (B-C). Met-1 tumor cells were injected alone or at a 1:1 ratio with UV irradiated iMEFs(D). Lungs were processed for microscopy and stained with anti-cleaved caspase-3 (A) or flow cytometry and stained with fluorescent Annexin V (AxV) and PI (B-D). Tumor cells expressed ZsGreen or GFP and were gated on as GFP+, CD45- population after excluding doublets and debris.

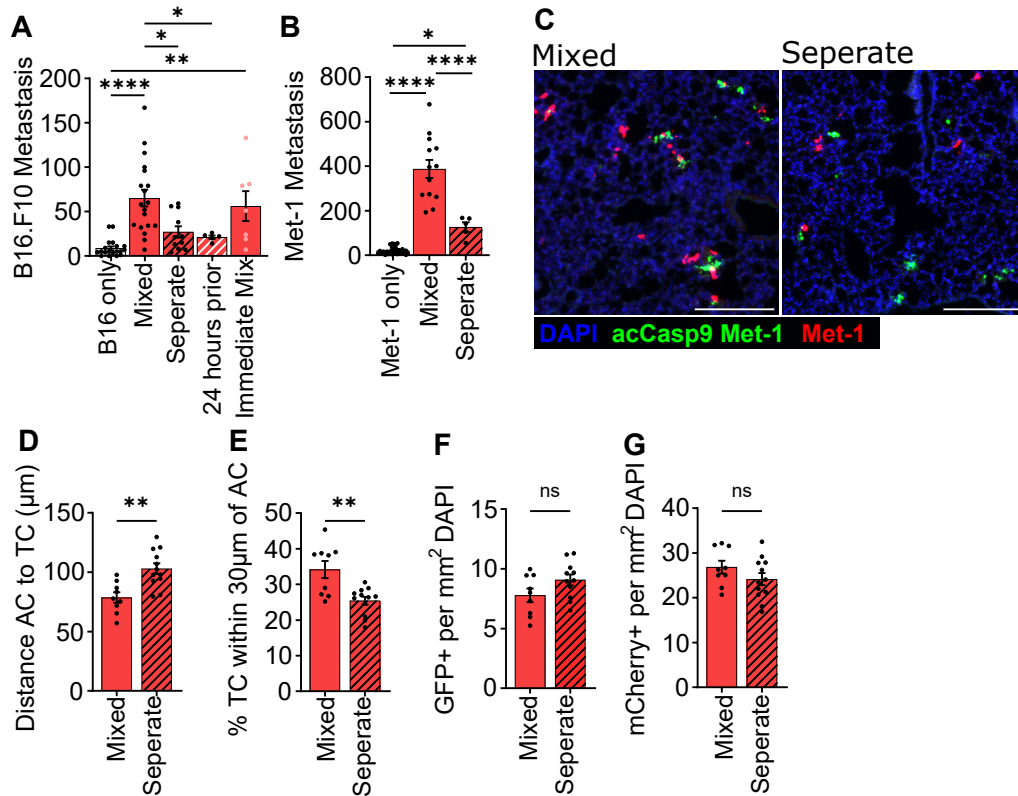


**Figure 5. Spatial association of apoptotic cells with tumor cells is necessary for apoptotic cells to exert their pro-metastatic effect.** B16.F10 (A) or Met-1 (B-G) cells were injected I.V. alone or in combination with acCasp8 3T3 (A-B). Tumor cells and apoptotic cells were mixed up to one hour in advance (mixed) or immediately prior and injected in a single bolus, or injected in two sequential injections into opposite tail veins (seperate), or apoptotic cells were injected 24 hours prior to tumor cell challenge. Surface lung metastasis was quantified after 14 days (A-B). Lungs were harvested 1 hour after I.V. for visualization by fluorescent microscopy, acCasp9 Met-1 cells were stained with CFSE (green) and Met-1 cells expressed mCherry (red), scale bar=200 $\mu\text{m}$  (C-G). Error bars represent SEM, Dots are biological replicates (A-B) or represent distinct slices of lung tissue taken from n=3-4 biological replicates (D-G), statistical testing is Ordinary one-way ANOVA with Tukey's multiple comparisons test (A-B) or unpaired t-test (D-G) AC=Apoptotic Cell, TC=Tumor Cell

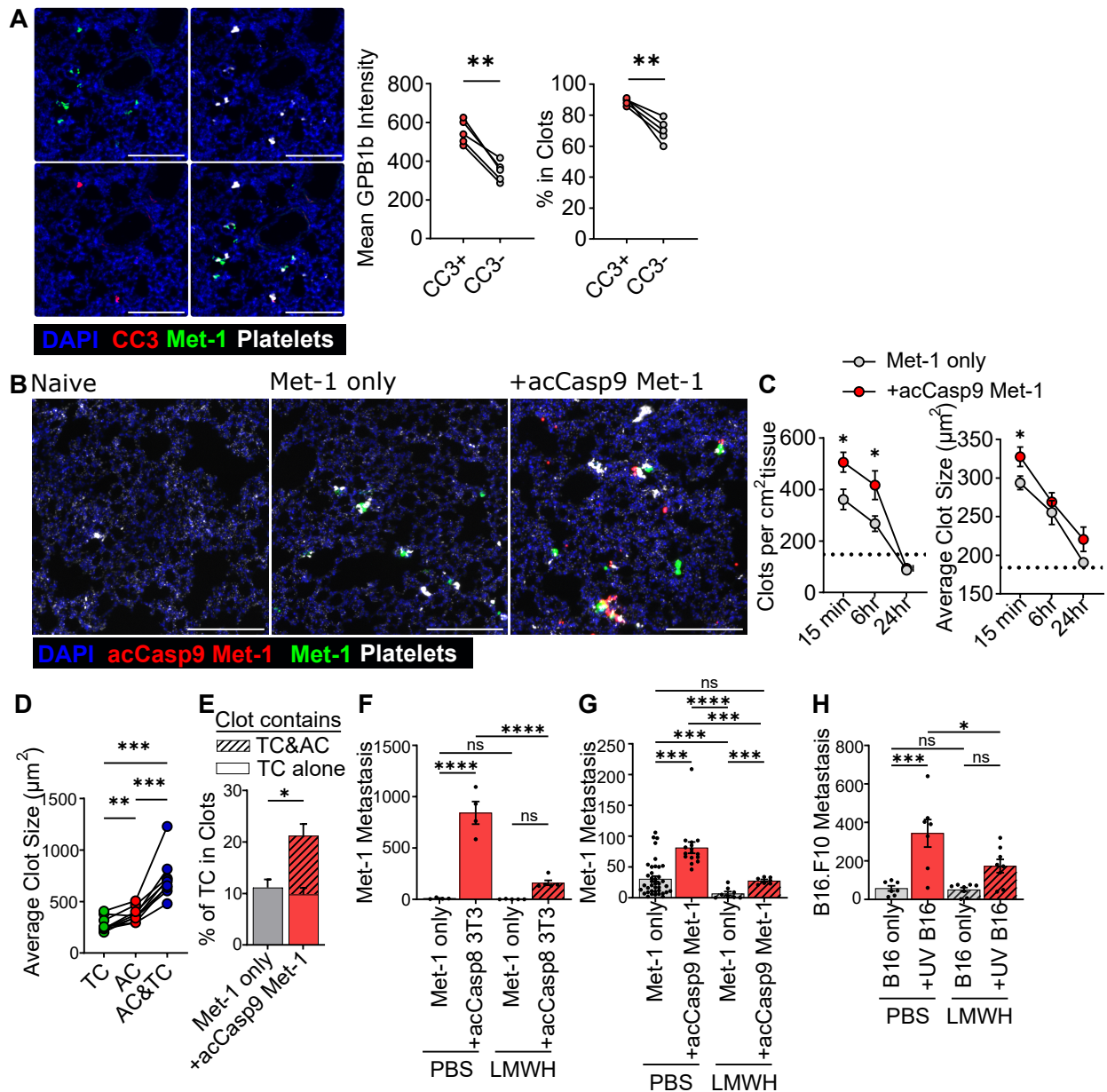


**Figure 6. Apoptotic cells promote platelet aggregation on tumor cells and the effect of apoptotic cells on metastasis depends on coagulation.** Met-1 cells were injected I.V. with acCasp9 Met-1 (A-E,G) or acCasp8 3T3 (F). B16.F10 cells were injected I.V. with UV irradiated B16.F10 cells (H). Low-molecular-weight heparin (LMWH) was administered s.c. at -4, 0, and 24 hours in relation to I.V. tumor cell injection (F-H). Lungs were harvested at 15 min (A-E) or indicated timepoints and processed for fluorescent imaging. Surface lung metastasis quantified after 14 days (F-G). Met-1 tumor cells expressed ZsGreen (green), apoptotic acCasp9 Met-1 expressed mCherry (red), platelets are stained with  $\alpha$ GPIIb $\beta$  (white), scale bar=200 $\mu$ m (A-E). Dotted line is the mean of naive lung controls (C). Average size of clots that contained either an Apoptotic cell (AC), Tumor cell (TC) or an AC and TC was quantified, lines connect values from individual lung sections (D). Striped portion of bar is the % of tumor cells in a clot that also contains an apoptotic cell (E). Error bars represent SEM, dots are multiple slices of lung from n=3-4 biological replicates (A-E) or dots are biological replicates (F-G). Analysis with unpaired T-tests (A-C,E) or by ordinary one-way ANOVA with Tukey's multiple comparisons test (D,F-G)

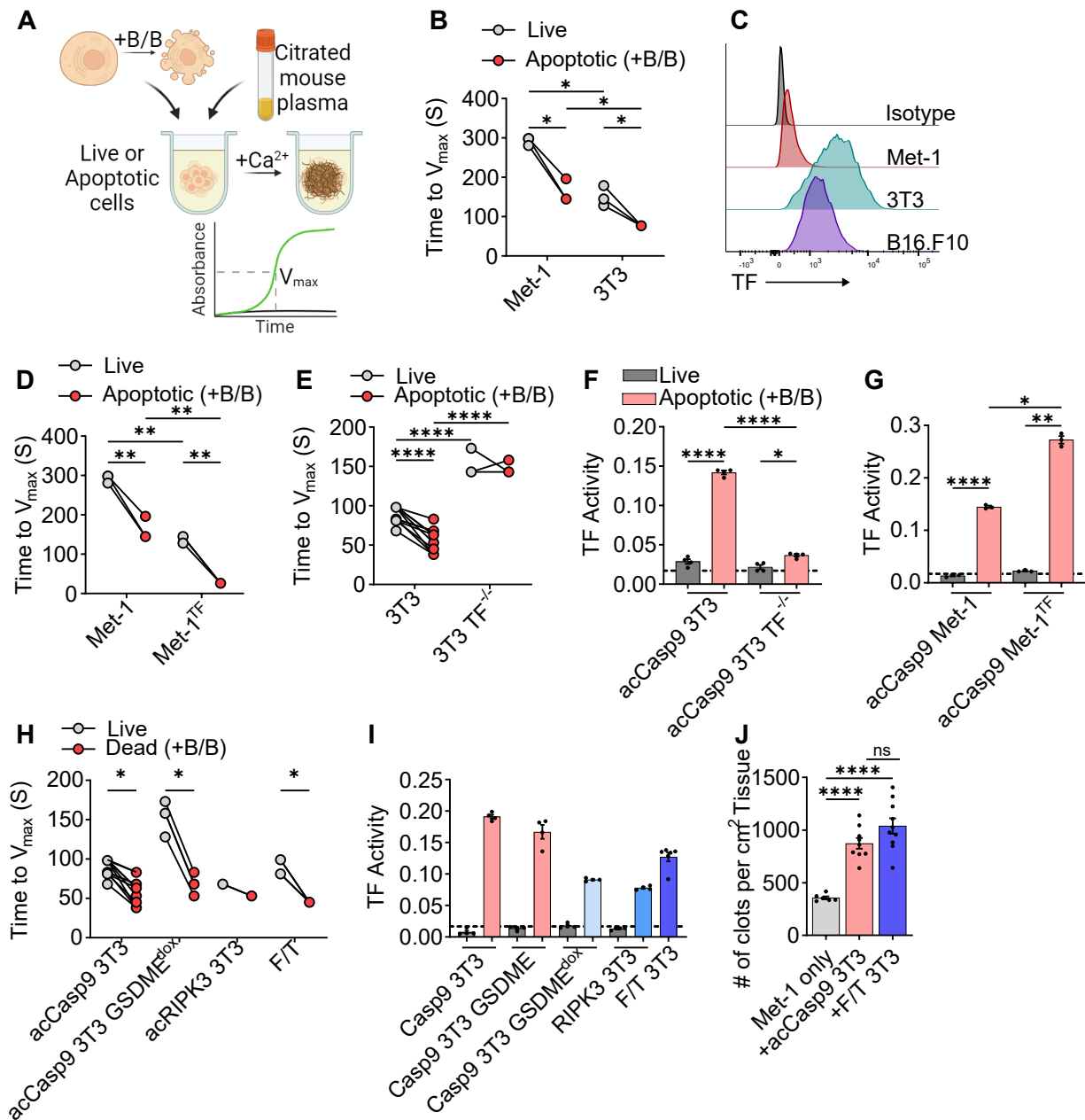


**Figure 7. Apoptotic cells have enhanced procoagulant activity** Time to fibrin clot formation was measured as the maximum change in absorbance (Time to  $V_{max}$ ) after adding  $Ca^{2+}$  to citrated mouse plasma containing live or apoptotic cells, lower values indicate more rapid clot formation (A,B,D,E,H). Met-1 or 3T3 were left untreated or treated with B/B for 2 hours (B,D-J). TF-PE fluorescent intensity was measured by flow cytometry (C). TF activity was measured as the absorbance at 30 minutes after addition of live or apoptotic cells to mouse FVII, human FX, and chromogenic FXa substrate (F,G,I). Lungs were harvested at 15 min after I.V. and processed for fluorescent imaging (J). Circles connected by lines are matched serum samples and statistical analysis is 2way ANOVA with Šidák multiple comparison test (B,D,E,H). Dotted line represents the absorbance of a control well containing all assay components without cells added, statistical analysis is Welch's ANOVA with Dunnett's multiple comparisons test, error bars represent SEM (F-G,I).

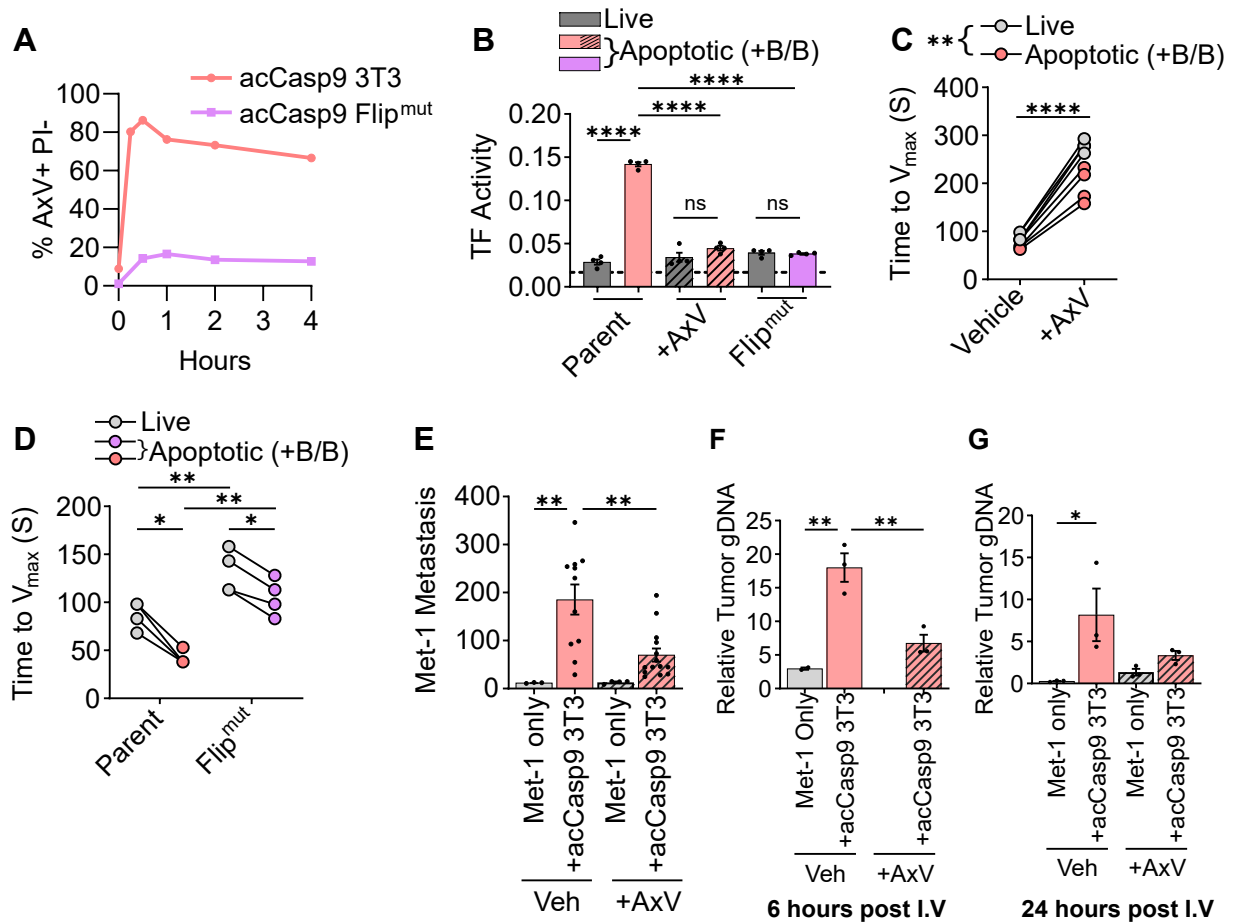


**Figure 8. Phosphatidylserine exposure promotes the coagulant activity of apoptotic cells.** acCasp9 3T3 were left untreated or treated with B/B for 2 hours (A-D) or 15 minutes (E-G). PS exposure was analyzed by flow cytometry at various timepoints (A). TF activity was measured as the absorbance at 30 minutes after addition of live or apoptotic cells to mouse FVII, human FX, and chromogenic FXa substrate (B). Time to fibrin clot formation was measured as the maximum change in absorbance (Time to  $V_{max}$ ) after adding  $Ca^{2+}$  to citrated mouse plasma containing live or apoptotic cells, lower values indicate more rapid clot formation (C-D). Annexin V (AxV) was added to cells in  $Ca^{2+}$  containing buffer and incubated on ice for 30 minutes (B,C,E). Surface lung metastasis was quantified at 14 days post I.V. injection (E). Lung gDNA was harvested at indicated timepoints for qPCR (F-G) Dotted line represents the absorbance of a control well containing all assay components without cells added (B). Statistical analysis is Welch's ANOVA with Dunnett's multiple comparisons test, error bars represent SEM (B,E-G). Circles connected by lines are matched serum samples and statistical analysis is 2way ANOVA with Šidák multiple comparison test (C,D).

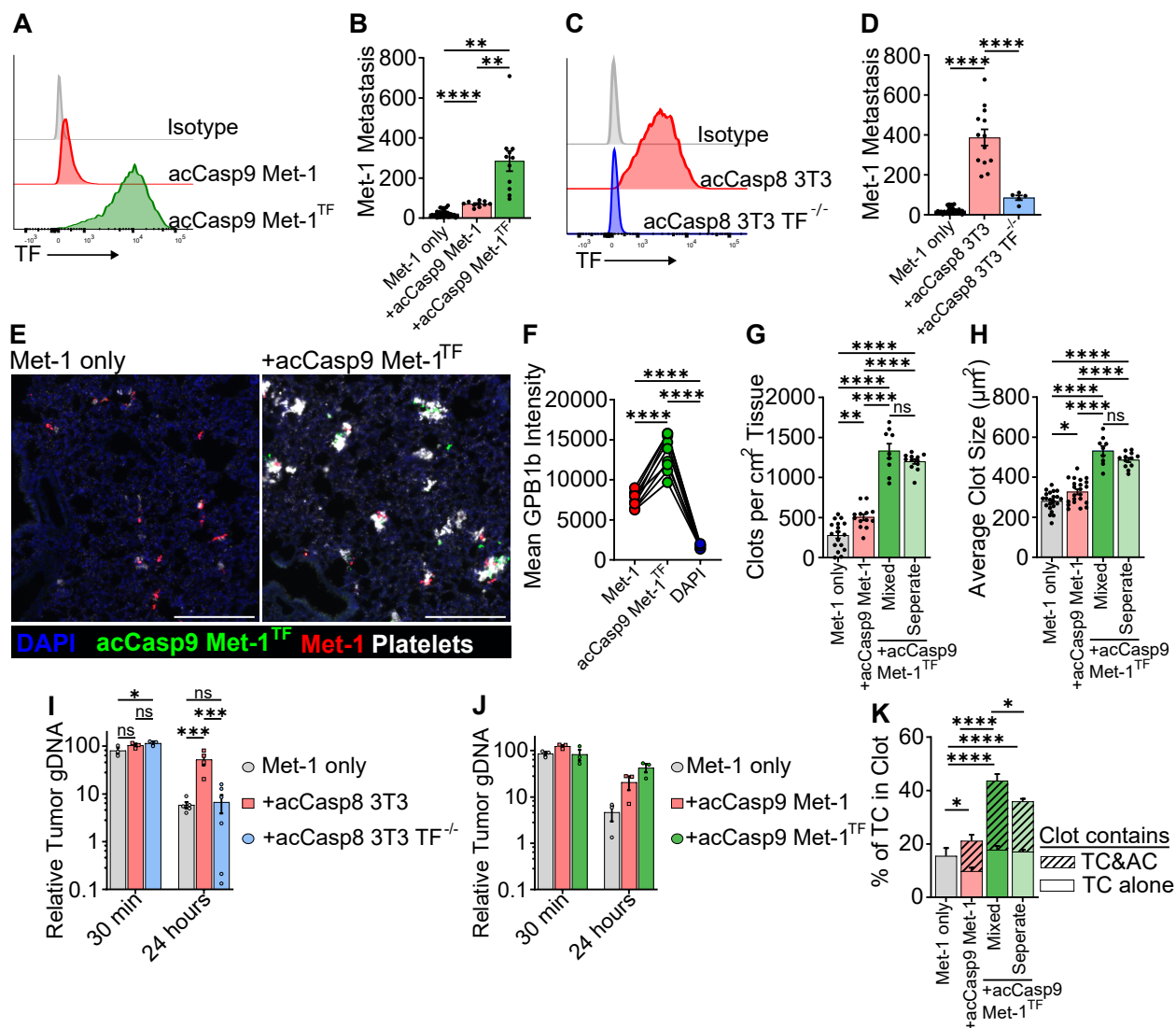


**Figure 9. Tissue Factor is responsible for the magnitude of apoptotic cell enhanced metastasis and platelet clotting in the lung.** TF was overexpressed on acCasp9 Met-1 cells or knocked out on acCasp8 3T3 cells. TF-PE fluorescent intensity was measured by flow cytometry on live cells (A,C). acCasp9 Met-1 (B,E-H,J-K) or acCasp8 3T3 (D,I) were treated with B/B for 15 minutes. Surface lung metastasis was quantified at 14 days post I.V. injection (B,D). Lungs were harvested for fluorescent microscopy 1 hour after I.V. injection, Met-1 and acCasp9 Met-1<sup>TF</sup> cells were mixed up to one hour in advance and injected in a single bolus (mixed), or injected in two sequential injections into opposite tail veins (separate), acCasp9 Met-1<sup>TF</sup> cells were stained with CFSE (green), Met-1 cells expressed mCherry (red), platelets are stained with αGP1bβ (white), scale bar=200μm (E-H,K). Lung gDNA was harvested at indicated timepoints for qPCR (I-J). Mean GPB1b intensity on Met-1 tumor cells, acCasp9 Met-1<sup>TF</sup> apoptotic cells, or across all DAPI+ tissue was quantified from mice that received Met-1 mixed with acCasp9 Met-1<sup>TF</sup>, lines connect values from individual lung sections (F). Striped portion of bar is the % of tumor cells in a clot that also contains an apoptotic cell (K). Dots are biological replicates (B,D,I,J) or multiple slices of lung from n=3-4 biological replicates (F-H). Statistical testing is Ordinary one-way ANOVA with Tu key's multiple comparisons test. Error bars represent SEM. AC=Apoptotic Cell, TC=Tumor Cell

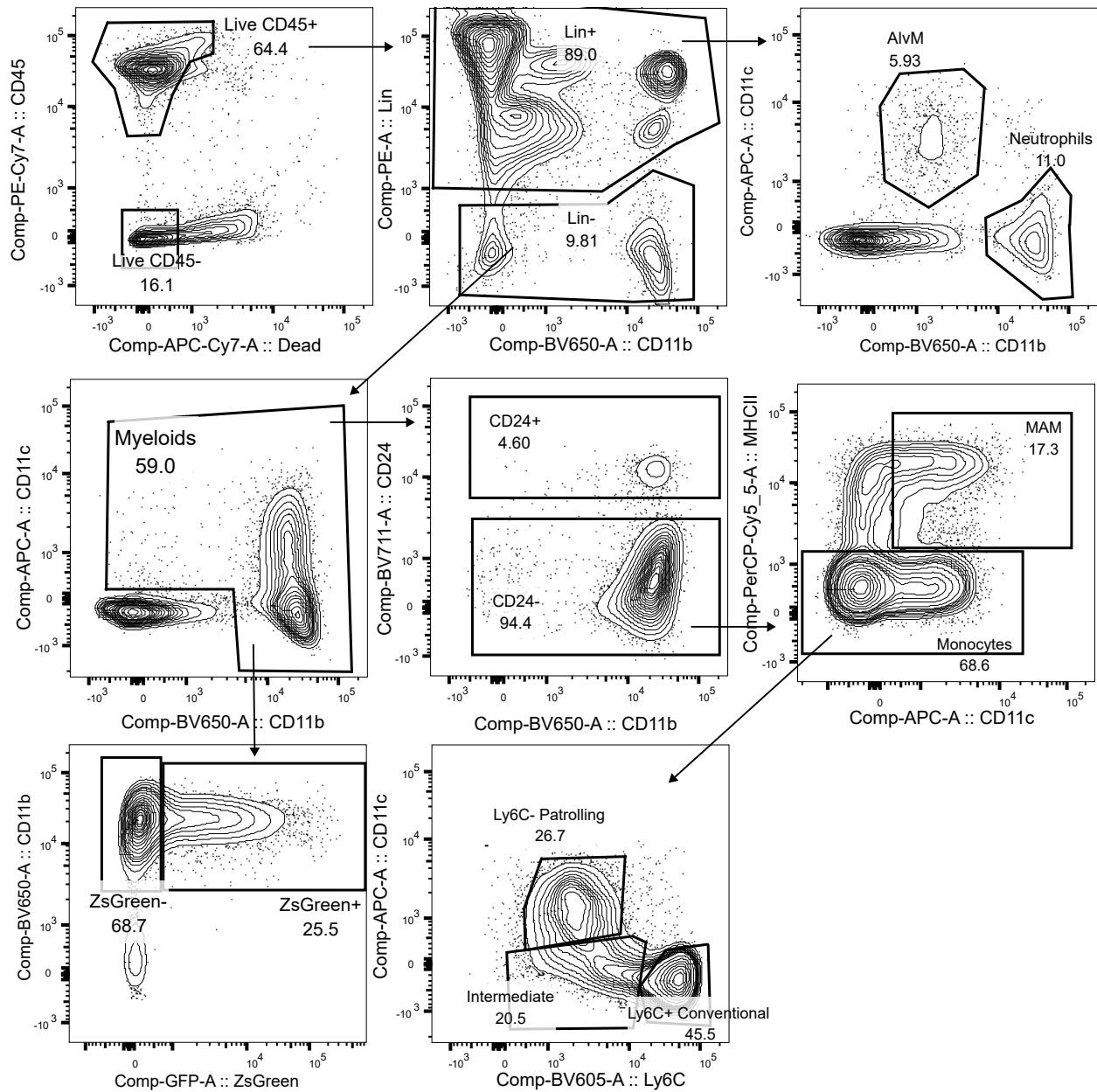
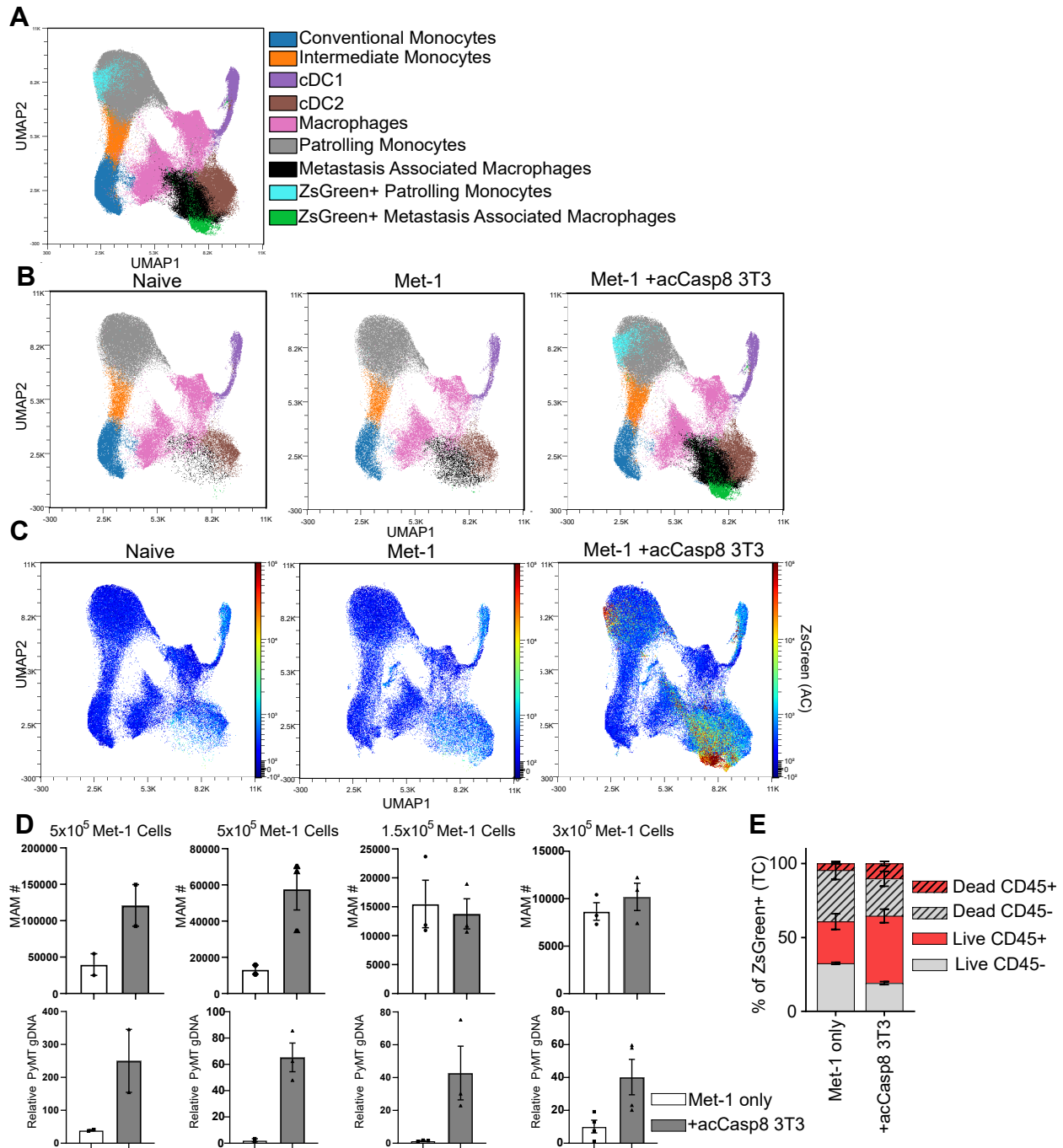
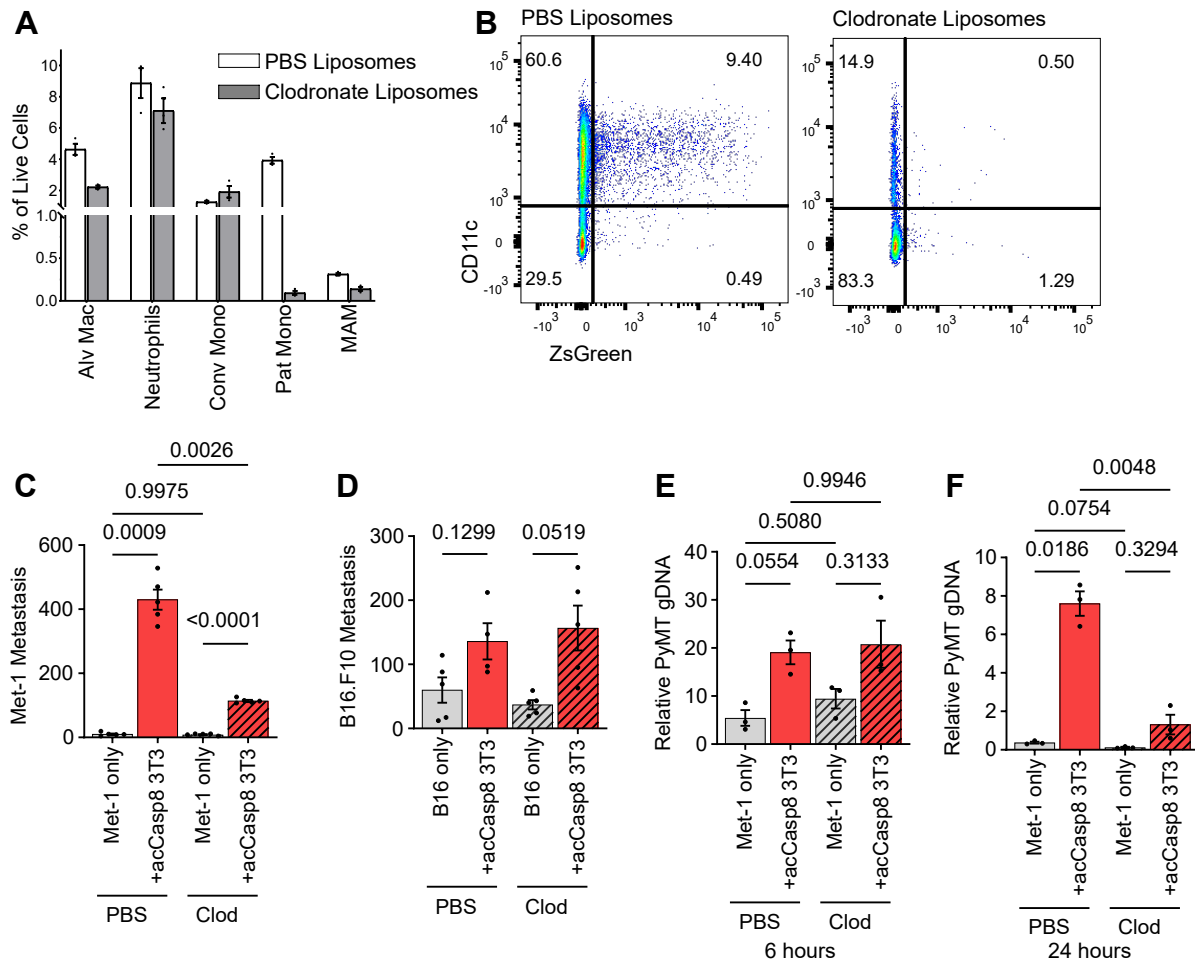


Figure 10. **Lung Myeloid Gating Scheme.** Lungs were harvested from mice at 24 hours following I.V. injection of ZsGreen expressing cells. Cells were first gated using FSC and SSC, the singlets gating before gating on myeloid populations as indicated.



**Figure 11. Metastasis Associated Macrophages are recruited to the lungs and phagocytose apoptotic material.** Lungs were harvested from mice at 24 hours following I.V. injection of ZsGreen expressing cells and processed for Flow Cytometry. Cells were gated as in Figure 10 and displayed in UMAP space. Columns are matched experimental repeats (D) MAMs were quantified by flow cytometry and gDNA was processed from the left lung lobe for qPCR quantification of tumor cell survival (lower half of panel D).



**Figure 12. Phagocyte depletion reduces metastasis in Met-1 model but not B16.F10**  
 Depletion of phagocytic populations was quantified by Flow Cytometry 24 hours after I.V. injection of tumor and ZsGreen expressing apoptotic cells (A-B). Surface metastasis was quantified 14 days after I.V. (C-D). Lung gDNA was processed at indicated timepoints and tumor cell quantity determined by qPCR (E-F) Statistical testing is Ordinary one-way ANOVA with Tukey's multiple comparisons test. Error bars represent SEM.

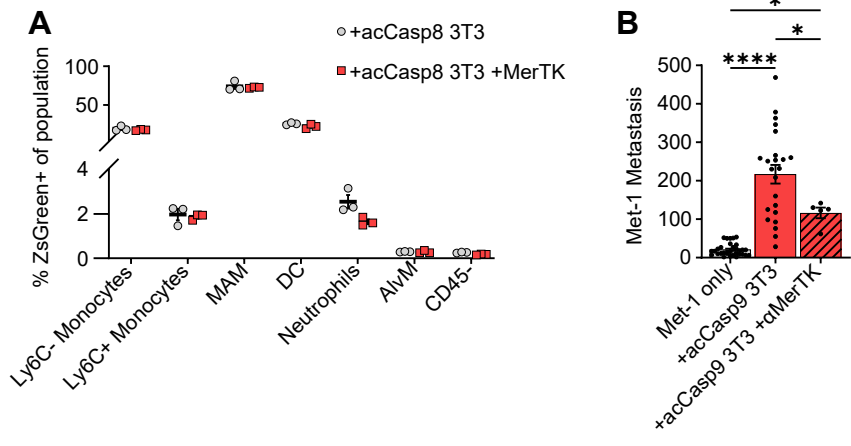


Figure 13. **MerTK blockade reduced metastasis but did not alter phagocytosis of apoptotic cells.** Uptake of ZsGreen+ apoptotic material by phagocytic populations was quantified by Flow Cytometry 24 hours after I.V. injection. (A) Surface metastasis was quantified 14 days after I.V. (B).

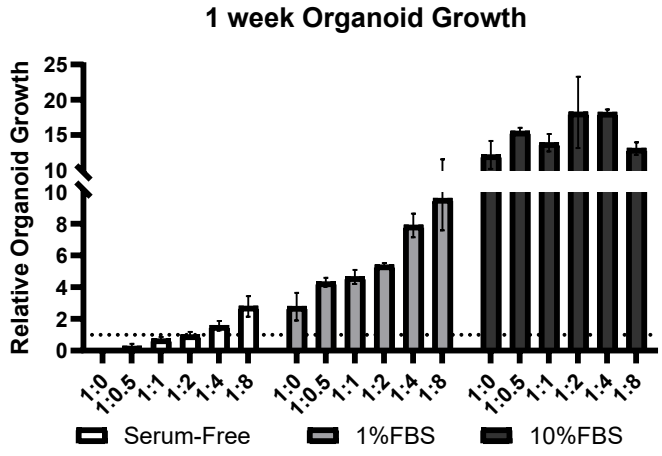


Figure 14. **Apoptotic cells enhance tumor organoid growth in low serum conditions.** Tumor cells were plated with increasing ratios of acCasp8 3T3 treated with B/B for 15 minutes in indicated concentrations of Fetal Bovine Serum (FBS). Organoid area was quantified after 7 days by Incucyte.

## Materials and Methods

**Sex as a biological variable-** Our study examined only female animals because breast cancer metastasis is a disease burden primarily in females. It is unknown whether the findings are relevant for male mice.

**Cell Culture-** Cell lines were cultured at 37C with 5% CO<sub>2</sub> in Dulbecco's modification of Eagle medium (DMEM) supplemented with 10% (v/v) fetal bovine serum (FBS), 2 mM l-glutamine, 10 mM HEPES, and 1 mM sodium pyruvate (complete DMEM). Cell lines were passaged every 1-3 days and used for experiments within 2 weeks after thawing from liquid nitrogen stocks. Cells were regularly tested and remained negative for mycoplasma contamination. Adherent cells were detached from plate using Trypsin-EDTA (0.25%). Mouse Embryonic Fibroblasts (MEFs) were derived from day 15.5 embryos of B6/J or FVB/N pregnant mice as previously described<sup>124</sup>. MEFs were immortalized by transforming with lentivirus containing SV40 Large T antigen (iMEF). B16-F10 (CRL-6475) and NIH/3T3 (CRL-1658) cells were purchased from ATCC. Met-1 cells were derived from mammary carcinomas in FVB/N-Tg(MMTV-PyVmT) and kindly provided by Dr. Alexander Borowsky<sup>53</sup>. Met-1<sup>TF</sup> cells were generated by lentiviral transformation with pCMV3-C-GFPspark containing the mouse Tissue factor ORF (SinoBiological). NIH/3T3 TF<sup>-/-</sup> cells were generated by lentiviral transformation with pRRL.U6.gRNA.MND.Cas9.2A.Hygro containing the guide RNA sequence CTCGTCTGTGAGGTCGCACT. Flip<sup>mut</sup> cells were generated by lentiviral transformation with pRRL.U6.gRNA.MND.Cas9.2A.Hygro containing the guide RNA sequence targeting *XKR8*, CGTACTGGACAACGGCCCAC, and pMX.puro containing a mutant of ATP11c with D to A mutations in the three caspase cleavage sites, kindly provided by Dr. Shigekazu Nagata<sup>20</sup>.

**Mice-** Female C57BL6/J (B6/J) mice and FVB/NJ mice (FVB) were purchased from the Jackson Laboratory and allowed to acclimate at least 1 week before experiment initiation. Experiments were performed on 6-10 week old mice. A *Rag2*<sup>-/-</sup> breeding pair was purchased from the Jackson Laboratory and bred in house for experiments. Mice were housed under specific pathogen-free conditions at the University of Washington. All animals were maintained according to protocols approved by the University of Washington Institutional Animal Care and Use Committee (IACUC), under protocol number 4298-01 (PI: AO).

**Cell Death Induction-** The activatable cell death systems have been described extensively previously<sup>54-57</sup>. Briefly, NIH/3T3 cell lines were transduced with lentiviral plasmid (pRRL) encoding activatable (“ac”) Caspase-8, Caspase-9 or RIPK3. pSLIK lentiviral vector was used for thyroid response element controlled expression of acCasp9 in B16-F10 and Met-1 cell lines and GSDME in NIH/3T3 cells. pSLIK gene expression was induced by culturing cells in doxycycline (1 µg/ml; Sigma-Aldrich) for 18 hours before harvesting for cell death induction. Programed cell death was induced by incubating cells in complete DMEM with 1 mM B/B homodimerizer (Clontech) for 15 min at 37°C. Cells were then washed with cold phosphate-buffered saline (PBS) before being resuspended in PBS at designated concentrations. Cells killed by freeze/thaw lysis were cycled between liquid nitrogen and a 37°C water bath 3 times<sup>58</sup>. Cells killed by UV irradiation were exposed to 100mj/cm<sup>2</sup> UV light using a UVP CL-1000 Ultraviolet Crosslinker. % Cell death was monitored using Sytox Green dye (Invitrogen) and Incucyte live cell imaging (Sartorius). Phosphatidylserine exposure was analyzed on a flow cytometer after staining cells with Fluorescent conjugated Annexin V (Invitrogen) and Propidium Iodide (Ebioscience) in Annexin Binding Buffer.

**Intravenous Metastasis-**  $1.5 \times 10^5$  Met-1 tumor cells or  $7 \times 10^4$  B16-F10 cells were suspended in PBS with an equivalent number of apoptotic cells. 100 $\mu$ L of this mixture was injected intravenously into the tail vein of mice after warming under a heat lamp for 5 minutes. B16-F10 metastasis were quantified 14 days after by counting black tumor nodules on the surface of all lung lobes, Met-1 metastasis was quantified by staining lung tissue with 15% India Ink intratracheally, then incubating lungs in Fekete's solution for 24 hours at 4°C before counting white tumor nodules on the surface of all lung lobes. For separate tail vein experiments apoptotic cells and tumor cells were suspended in PBS and 100 $\mu$ L of each cell type was injected into the left and right tail veins respectively. For phosphatidylserine blocking, 25 $\mu$ g/mL purified Annexin V (Biolegend) was added to cells in HBSS+Ca<sup>2+</sup>+Mg<sup>2+</sup>.

**Heparin Treatment-** 200 $\mu$ g of low molecular weight heparin, Enoxaparin sodium (Sigma Aldrich) dissolved in 200 $\mu$ L PBS was injected subcutaneously into the flank of mice at hours -4, 0 and 24 relative to I.V. tumor cell injection.

**NK cell depletion-** Mice were administered 200 $\mu$ g anti-NK1.1 clone PK136 (Bio X Cell) or isotype mouse IgG2a clone C1.18.4 (Bio X Cell) in 200  $\mu$ L PBS intraperitoneally at 72 and 24 hours prior to I.V. metastasis challenge.

**MerTK Treatment-** Mice were administered 400 $\mu$ g anti-MerTK mIgG2a LALAPG antibody<sup>117</sup> (Genentech) in 200 $\mu$ L PBS intraperitoneally 1 hour prior to I.V. metastasis challenge.

**Clodronate Treatment-** Mice were anesthetized with isoflurane. 150 $\mu$ L of Clodronate or PBS control liposomes were injected retro-orbital at days -3, -1 and 1 relative to I.V. tumor cell injection.

**Quantification of injected cell genomic DNA in Lung-** The left lobe was dissected, rinsed in PBS, and placed in 1mL DNAzol (Invitrogen). The tissue was homogenized using Precellys Tissue Homogenizer with ceramic beads. Genomic DNA was isolated from homogenate according to the DNAzol reagent manual. The concentration of genomic DNA isolated was quantified using spectrophotometer and concentrations were normalized by diluting samples in nuclease-free water. Quantitative Taqman probe based PCR was used to quantify the PyMT transgene or other ectopically expressed transgenes (ZsGreen, GFP, mCherry). Primer/Probe sequences listed in the table below. The relative abundance of target genes was calculated as  $2^{-\Delta\Delta CT}$  where  $\Delta CT = CT^{\text{Target}} - CT^{\text{ptger2}}$  and  $\Delta\Delta CT = \Delta CT^{\text{sample}} - \text{Average } \Delta CT^{\text{initial}}$ .

Target	Fwd Primer	Rev Primer	FAM/NFQ-MGB Probe
<b>Ptger2</b> (To detect total Murine gDNA)	TAC CTT CAG CTG TAC GCC AC	GCC AGG AGA ATG AGG TGG TC	/56-FAM/CC TGC TGC T/ZEN/T ATC GTG GCT G/3IABkFQ/
<b>ZsGreen</b> (To detect cells cells expressing ZsGreen)	GTA CCA CGA GTC CAA GTT CTA C	CAC GTC GCC CTT CAA GAT	/56-FAM/CC CGT GAT G/ZEN/A AGA AGA TGA CCG ACA A/3IABkFQ/
<b>PyMT</b> (To detect cells from MMTV-PyMT Mouse, i.e. Met-1 cells)	CGA AAT CCT TGT GTT GCT GA	GCT GGT CTT GGT CGC TTT C	/56-FAM/CC GAT GAC A/ZEN/G CAT ATC CCC /3IABkFQ/
<b>mCherry</b> (To detect cells expressing mCherry)	GAC TAC TTG AAG CTG TCC TTC C	CGC AGC TTC ACC TTG TAG AT	/56-FAM/TT CAA GTG G/ZEN/G AGC GCG TGA TGA A/3IABkFQ/
<b>GFP</b> (To detect cells expressing GFP)	GAA CCG CAT CGA GCT GAA	TGC TTG TCG GCC ATG ATA TAG	/56-FAM/AT CGA CTT C/ZEN/A AGG AGG ACG GCA AC/3IABkFQ/
<b>101a</b> (To detect cells with 101a heterodimerizer)	GAG GAG ACT GTA CGC AAG ATG	TGG CGC TGC TGT TTG ATA	/56-FAM/AT CAC CAC C/ZEN/T TCA CCT CGT TGC C/3IABkFQ/
<b>SV40 Large T</b> (To detect immortalized MEFs)	GTG GCA TTG CTT TGC TTC TTA	GTC CAA TCT CTC TTT CCA CTC C	/56-FAM/AG ACC TGT G/ZEN/G CTG AGT TTG CTC AA/3IABkFQ/

**Flow Cytometry-** Lungs were rinsed in PBS, roughly dissociated with scissors, then incubated with 50 $\mu$ g/mL Liberase TM (Sigma), 250 $\mu$ g/mL DNase I (Sigma) in HBSS with Ca<sup>2+</sup> & Mg<sup>2+</sup> for 35 minutes at 37C with gentle agitation. Tissue was homogenized with

GentleMACS lung dissociation (Miltenyi Biotec) and strained through 70 $\mu$ m cell strainers. Single cell suspensions were stained with fluorochrome conjugated antibodies in PBS with 3% FBS +0.05% NaAzide. Antibodies used are CD45 clone 30-F11 (Biolegend), Tissue factor polyclonal (R&D Systems), CD3 clone 145-2C11 (BD Bioscience), NKp46 clone PK136 (Biolegend). Fluorescent conjugated Annexin V (Invitrogen) and Propidium Iodide (Ebioscience) staining was added to cells suspended in Annexin Binding Buffer prior to running on either a CantoRUO or Symphony flow cytometer (BD Biosciences). Data was analyzed with FlowJo software (TreeStar).

**Immunofluorescent imaging-** Mouse lung tissue was fixed in a 1:3 dilution of Cytotfix fixation buffer (BD) in PBS for 18 hours, washed with PBS twice, then embedded in OCT medium and frozen. In some experiments, cells were stained with CFSE (Invitrogen) prior to injection. 20 $\mu$ m slices were prepared with a Cyrostat on glass microscope slides and stained with primary and secondary antibodies in 1%BSA in PBT (PBS with 0.1% Triton X-1000) after blocking with 10% BSA in PBT. Antibodies used were anti-GPIIb $\beta$  conjugated to Dylight 649 (X649, Emfret analytics); and rabbit anti-mCherry polyclonal (Rockland). Slides were mounted with Aqua-mount (Epreidia) and images were acquired on a Leica DMI6000 inverted microscope with 10X LWD dry objective and Leica DFC365 FX CCD camera. LASX software was used for image acquisition and mosaic tiling.

**Image analysis-** ImageJ was used to quantify platelet clots, tumor cell numbers, and apoptotic cell numbers. Positive staining was defined using manual thresholding. Clots, tumor cells, and apoptotic cells were defined as stain positive objects  $>200\mu\text{m}^2$ . QuPath was used to quantify spatial parameters such as colocalization of cell within clots and distances between cells using manual thresholding to define objects.

**Plasma Coagulation Assay-** Blood was drawn from the left ventricle into syringes containing citrate-dextrose solution (Sigma-Aldrich) at a dilution of 9:1. Platelet-poor plasma was isolated after two sequential centrifugations at 5,000xg for 10 minutes. Plasma was stored at -80 and thawed only once before use in assay. All reagents were brought to 37°C for assay. 50µL citrated platelet-poor plasma was aliquoted into wells of a 96 well polystyrene plate. 100,000 cells were added to wells in 50µL PBS. 50µL of 25mM CaCl<sub>2</sub> was added to allow the coagulation reaction to occur. Absorbance at 405nm was measured every 15 seconds by the Synergy HT microplate reader at 37°C with a 2 second shaking step in between each read. The time to the maximum change in absorbance was calculated (Time to V<sub>max</sub>).

**Tissue factor activity assay-** Live cells or cells stimulated to undergo apoptosis (20,000 per well) were added to a 96 well plate. HEPES buffered saline with BSA (1mg/mL) containing 0.6nM Mouse Factor VII (Biotechne), 125nM Human Factor X (Prolytix), and 150µM Factor Xa chromogenic substrate (Sigma-Aldrich) was added to each well. Absorbance at 405nm was read every 3 minutes on a Biotek Synergy HTX microplate reader set to 37°C with a shaking step before each reading. Absorbance readings were blanked to the absorbance of the well at 0 minutes.

**Tumor Organoid Assay-** a 96-well flat bottom polystyrene plate was coated with matrigel dilute with cell culture media with 10%, 1% or 0% FBS supplementation. After allowing the matrigel to solidify for 30 minutes at 37°C, 5x10<sup>3</sup> Met-1 tumor cells were plated on top, alone or with increasing ratios of apoptotic cells in 100µL cell culture media with 10%, 1% or 0% FBS supplementation. Tumor Organoids were imaged every 4 hours using the Incucyte live cell imaging (Sartorius) using the Multi-Spheroid module.

**Statistics-** GraphPad Prism was used to calculate statistical significance. Statistical tests are indicated in the figure legends. \*,\*\*,\*\*\*,\*\*\*\* corresponds to  $0.01 > P > 0.05$ ,  $0.001 > P > 0.01$ ,  $0.0001 > P > 0.001$ ,  $P < 0.0001$  respectively.

**Study approval-** All procedures and use of animals was approved by the University of Washington IACUC.

**Data and material availability-** Values for all figures can be found in the supplemental data values file. Reagents described in this manuscript are available from A.O. for research use under a materials transfer agreement from the University of Washington.

## References

1. Ucker DS, Levine JS. Exploitation of Apoptotic Regulation in Cancer. *Front Immunol*. 2018;9:241. doi:10.3389/fimmu.2018.00241
2. Naresh KN, Lakshminarayanan K, Pai SA, Borges AM. Apoptosis index is a predictor of metastatic phenotype in patients with early stage squamous carcinoma of the tongue: A hypothesis to support this paradoxical association. *Cancer*. 2001;91(3):578-584. doi:10.1002/1097-0142(20010201)91:3<578::AID-CNCR1037>3.0.CO;2-W
3. Jalali Nadoushan M, Peivareh H, Azizzadeh Delshad A. Correlation between Apoptosis and Histological Grade of Transitional Cell Carcinoma of Urinary Bladder. *Urol Oncol*. 2004;1(3):177-179.
4. Sun B, Sun Y, Wang J, Zhao X, Wang X, Hao X. Extent, relationship and prognostic significance of apoptosis and cell proliferation in synovial sarcoma. *Eur J Cancer Prev*. 2006;15(3):258-265. doi:10.1097/01.cej.0000198896.02185.68
5. de Jong J, van Diest P, Baak J. Number of apoptotic cells as a prognostic marker in invasive breast cancer. *Br J Cancer*. 2000;82:368-373.
6. Alcaide J, Funez R, Rueda A, et al. The role and prognostic value of apoptosis in colorectal carcinoma. *BMC Clin Pathol*. 2013;13(1):24. doi:10.1186/1472-6890-13-24
7. Ito Y, Matsuura N, Sakon M, et al. Both cell proliferation and apoptosis significantly predict shortened disease-free survival in hepatocellular carcinoma. *Br J Cancer*. 1999;81(4):747-751. doi:10.1038/sj.bjc.6690758
8. Ichim G, Tait SWG. A fate worse than death: Apoptosis as an oncogenic process. *Nat Rev Cancer*. 2016;16(8):539-548. doi:10.1038/nrc.2016.58
9. Marusyk A, Porter CC, Zaberezhnyy V, DeGregori J. Irradiation Selects for p53-Deficient

- Hematopoietic Progenitors. Kemp C, ed. *PLoS Biol.* 2010;8(3):e1000324.  
doi:10.1371/journal.pbio.1000324
10. Huang Q, Li F, Liu X, et al. Caspase 3-mediated stimulation of tumor cell repopulation during cancer radiotherapy. *Nat Med.* 2011;17(7):860-866. doi:10.1038/nm.2385
  11. Ford CA, Petrova S, Pound JD, et al. Oncogenic properties of apoptotic tumor cells in aggressive B cell lymphoma. *Curr Biol.* 2015;25(5):577-588.  
doi:10.1016/j.cub.2014.12.059
  12. Douglas R. Green. *Cell Death: Apoptosis and Other Means to an End, Second Edition.* 2nd editio. Cold Spring Harbor Laboratory Press; 2018.
  13. Elmore S. Apoptosis: A Review of Programmed Cell Death. *Toxicol Pathol.* 2007;35(4):495-516. doi:10.1080/01926230701320337
  14. Youle RJ, Strasser A. The BCL-2 protein family: Opposing activities that mediate cell death. *Nat Rev Mol Cell Biol.* 2008;9(1):47-59. doi:10.1038/nrm2308
  15. Green DR. The Death Receptor Pathway of Apoptosis. *Cold Spring Harb Perspect Biol.* 2022;14(2):1-12. doi:10.1101/cshperspect.a041053
  16. Taylor RC, Cullen SP, Martin SJ. Apoptosis: Controlled demolition at the cellular level. *Nat Rev Mol Cell Biol.* 2008;9(3):231-241. doi:10.1038/nrm2312
  17. Nagata S. Apoptosis and Clearance of Apoptotic Cells. *Annu Rev Immunol.* 2018;36(1):489-517. doi:10.1146/annurev-immunol-042617-053010
  18. Medina CB, Ravichandran KS. Do not let death do us part: “Find-me” signals in communication between dying cells and the phagocytes. *Cell Death Differ.* 2016;23(6):979-989. doi:10.1038/cdd.2016.13
  19. Suzuki J, Denning DP, Imanishi E, Horvitz HR, Nagata S. Xk-related protein 8 and CED-

- 8 promote phosphatidylserine exposure in apoptotic cells. *Science (80- )*. 2013;341(6144):403-406. doi:10.1126/science.1236758
20. Segawa K, Kurata S, Yanagihashi Y, Brummelkamp TR, Matsuda F, Nagata S. Caspase-mediated cleavage of phospholipid flippase for apoptotic phosphatidylserine exposure. *Science (80- )*. 2014;344(6188):1164-1168. doi:10.1126/science.1252809
21. Birge RB, Boeltz S, Kumar S, et al. Phosphatidylserine is a global immunosuppressive signal in efferocytosis, infectious disease, and cancer. *Cell Death Differ*. 2016;23(6):962-978. doi:10.1038/cdd.2016.11
22. Rogers C, Fernandes-Alnemri T, Mayes L, Alnemri D, Cingolani G, Alnemri ES. Cleavage of DFNA5 by caspase-3 during apoptosis mediates progression to secondary necrotic/pyroptotic cell death. *Nat Commun*. 2017;8:1-14. doi:10.1038/ncomms14128
23. Zhang Z, Zhang Y, Xia S, et al. Gasdermin E suppresses tumour growth by activating anti-tumour immunity. *Nature*. 2020;579(7799):415-420. doi:10.1038/s41586-020-2071-9
24. Nagata S. Apoptosis and autoimmune diseases. *Ann N Y Acad Sci*. 2010;1209(1):10-16. doi:10.1111/j.1749-6632.2010.05749.x
25. Dillekås H, Rogers MS, Straume O. Are 90% of deaths from cancer caused by metastases? *Cancer Med*. 2019;8(12):5574-5576. doi:10.1002/cam4.2474
26. Kitamura T, Qian B-Z, Pollard JW. Immune cell promotion of metastasis. *Nat Rev Immunol*. 2015;15(2):73-86. doi:10.1038/nri3789
27. Stanford JC, Young C, Hicks D, et al. Efferocytosis produces a prometastatic landscape during postpartum mammary gland involution. *J Clin Invest*. 2014;124(11):4737-4752. doi:10.1172/JCI76375
28. Furlow PW, Zhang S, Soong TD, et al. Mechanosensitive pannexin-1 channels mediate

- microvascular metastatic cell survival. *Nat Cell Biol.* 2015;17(7):943-952.  
doi:10.1038/ncb3194
29. Headley MB, Bins A, Nip A, et al. Visualization of immediate immune responses to pioneer metastatic cells in the lung. *Nature.* 2016;531(7595):513-517.  
doi:10.1038/nature16985
30. Gil-Bernabé AM, Ferjančič Š, Tlalka M, et al. Recruitment of monocytes/macrophages by tissue factor-mediated coagulation is essential for metastatic cell survival and premetastatic niche establishment in mice. *Blood.* 2012;119(13):3164-3175.  
doi:10.1182/blood-2011-08-376426
31. Gay LJ, Felding-Habermann B. Contribution of platelets to tumour metastasis. *Nat Rev Cancer.* 2011;11(2):123-134. doi:10.1038/nrc3004
32. Gil-Bernabé AM, Lucotti S, Muschel RJ. Coagulation And Metastasis: What Does The Experimental Literature Tell Us? *Br J Haematol.* 2013;162(4):433-441.  
doi:10.1111/bjh.12381
33. Lucotti S, Muschel RJ. Platelets and Metastasis: New Implications of an Old Interplay. *Front Oncol.* 2020;10:1350. doi:10.3389/fonc.2020.01350
34. Egan K, Cooke N, Kenny D. Living in shear: platelets protect cancer cells from shear induced damage. *Clin Exp Metastasis.* 2014;31(6):697-704. doi:10.1007/s10585-014-9660-7
35. Palumbo JS, Talmage KE, Massari J V., et al. Platelets and fibrin(ogen) increase metastatic potential by impeding natural killer cell-mediated elimination of tumor cells. *Blood.* 2005;105(1):178-185. doi:10.1182/blood-2004-06-2272
36. Ló Pez-Soto A, Gonzalez S, Smyth MJ, Galluzzi L. Control of Metastasis by NK Cells.

2017. doi:10.1016/j.ccell.2017.06.009
37. Placke T, Örgel M, Schaller M, et al. Platelet-derived MHC class I confers a pseudonormal phenotype to cancer cells that subverts the antitumor reactivity of natural killer immune cells. *Cancer Res.* 2012;72(2):440-448. doi:10.1158/0008-5472.CAN-11-1872
  38. Labelle M, Begum S, Hynes RO. Platelets guide the formation of early metastatic niches. *Proc Natl Acad Sci U S A.* 2014;111(30):E3053-E3061. doi:10.1073/pnas.1411082111
  39. Yang L, Liu Q, Zhang X, et al. DNA of neutrophil extracellular traps promotes cancer metastasis via CCDC25. *Nature.* 2020;583(7814):133-138. doi:10.1038/s41586-020-2394-6
  40. Szczerba BM, Castro-giner F, Vetter M, et al. Neutrophils escort circulating tumour cells to enable cell cycle progression. *Nature.* doi:10.1038/s41586-019-0915-y
  41. Spiegel A, Brooks MW, Houshyar S, et al. Neutrophils Suppress Intraluminal NK Cell-Mediated Tumor Cell Clearance and Enhance Extravasation of Disseminated Carcinoma Cells. 2016. doi:10.1158/2159-8290.CD-15-1157
  42. Gil-Bernabé AM, Ferjančič Š, Tlalka M, et al. Recruitment of monocytes/macrophages by tissue factor-mediated coagulation is essential for metastatic cell survival and premetastatic niche establishment in mice. *Blood.* 2012;119(13):3164-3175. doi:10.1182/blood-2011-08-376426
  43. Qian B, Deng Y, Im JH, et al. A Distinct Macrophage Population Mediates Metastatic Breast Cancer Cell Extravasation, Establishment and Growth. Bereswill S, ed. *PLoS One.* 2009;4(8):e6562. doi:10.1371/journal.pone.0006562
  44. Qian B-Z, Li J, Zhang H, et al. CCL2 recruits inflammatory monocytes to facilitate breast-

- tumour metastasis. *Nature*. 2011;475(7355):222-225. doi:10.1038/nature10138
45. Schumacher D, Strilic B, Sivaraj KK, Wettschureck N, Offermanns S. Platelet-Derived Nucleotides Promote Tumor-Cell Transendothelial Migration and Metastasis via P2Y2 Receptor. *Cancer Cell*. 2013;24(1):130-137. doi:10.1016/j.ccr.2013.05.008
  46. Summers MA, McDonald MM, Croucher PI. Cancer cell dormancy in metastasis. *Cold Spring Harb Perspect Med*. 2020;10(4):1-9. doi:10.1101/cshperspect.a037556
  47. Fidler IJ. Metastasis : Quantitative Analysis of Distribution and Fate of Tumor Emboli Labeled With 1-5-Iodo-2 ' -deoxyuridine. *J Natl Cancer Inst*. 1970;45(4):773-782.
  48. Grigoryeva ES, Tashireva LA, Alifanov V V., et al. The Novel Association of Early Apoptotic Circulating Tumor Cells with Treatment Outcomes in Breast Cancer Patients. *Int J Mol Sci*. 2022;23(16). doi:10.3390/ijms23169475
  49. Jansson S, Bendahl PO, Larsson AM, Aaltonen KE, Rydén L. Prognostic impact of circulating tumor cell apoptosis and clusters in serial blood samples from patients with metastatic breast cancer in a prospective observational cohort. *BMC Cancer*. 2016;16(1):433. doi:10.1186/s12885-016-2406-y
  50. Méhes G, Witt A, Kubista E, Ambros PF. Circulating breast cancer cells are frequently apoptotic. *Am J Pathol*. 2001;159(1):17-20. doi:10.1016/S0002-9440(10)61667-7
  51. Kallergi G, Konstantinidis G, Markomanolaki H, et al. Apoptotic Circulating Tumor Cells in Early and Metastatic Breast Cancer Patients. *Mol Cancer Ther*. 2013;12(9):1886-1895. doi:10.1158/1535-7163.MCT-12-1167
  52. Hou JM, Krebs MG, Lancashire L, et al. Clinical significance and molecular characteristics of circulating tumor cells and circulating tumor microemboli in patients with small-cell lung cancer. *J Clin Oncol*. 2012;30(5):525-532.

doi:10.1200/JCO.2010.33.3716

53. AD B, R N, LJ Y, et al. Syngeneic mouse mammary carcinoma cell lines: two closely related cell lines with divergent metastatic behavior. *Clin Exp Metastasis*. 2005;22(1):47-59. doi:10.1007/S10585-005-2908-5
54. Yatim N, Jusforgues-Saklani H, Orozco S, et al. RIPK1 and NF- $\kappa$ B signaling in dying cells determines cross-priming of CD8<sup>+</sup> T cells. *Science*. 2015;350(6258):328-334. doi:10.1126/science.aad0395
55. Snyder AG, Hubbard NW, Messmer MN, et al. Intratumoral activation of the necroptotic pathway components RIPK1 and RIPK3 potentiates antitumor immunity. *Sci Immunol*. 2019;4(36):2004. doi:10.1126/sciimmunol.aaw2004
56. Orozco SL, Daniels BP, Yatim N, et al. RIPK3 Activation Leads to Cytokine Synthesis that Continues after Loss of Cell Membrane Integrity. *Cell Rep*. 2019;28(9):2275-2287.e5. doi:10.1016/j.celrep.2019.07.077
57. Orozco S, Yatim N, Werner MR, et al. RIPK1 both positively and negatively regulates RIPK3 oligomerization and necroptosis. *Cell Death Differ*. 2014;21(10):1511-1521. doi:10.1038/cdd.2014.76
58. Basu S, Binder RJ, Suto R, Anderson KM, Srivastava PK. Necrotic but not apoptotic cell death releases heat shock proteins, which deliver a partial maturation signal to dendritic cells and activate the NF- $\kappa$ B pathway. *Int Immunol*. 2000;12(11):1539-1546. doi:10.1093/intimm/12.11.1539
59. Ichise H, Tsukamoto S, Hirashima T, et al. Functional visualization of NK cell-mediated killing of metastatic single tumor cells. *Elife*. 2022;11:1-28. doi:10.7554/ELIFE.76269
60. Chan IS, Ewald AJ. The changing role of natural killer cells in cancer metastasis. *J Clin*

- Invest.* 2022;132(6):1-9. doi:10.1172/JCI143762
61. Kim S, Iizuka K, Aguila HL, Weissman IL, Yokoyama WM. In vivo natural killer cell activities revealed by natural killer cell-deficient mice. *Proc Natl Acad Sci U S A.* 2000;97(6):2731-2736. doi:10.1073/pnas.050588297
  62. Cheung KJ, Padmanaban V, Silvestri V, et al. Polyclonal breast cancer metastases arise from collective dissemination of keratin 14-expressing tumor cell clusters. *Proc Natl Acad Sci U S A.* 2016;113(7):E854-E863. doi:10.1073/pnas.1508541113
  63. Aceto N, Bardia A, Miyamoto DT, et al. Circulating tumor cell clusters are oligoclonal precursors of breast cancer metastasis. *Cell.* 2014;158(5):1110-1122. doi:10.1016/j.cell.2014.07.013
  64. Knust J, Ochs M, Gundersen HJG, Nyengaard JR. Stereological estimates of alveolar number and size and capillary length and surface area in mice lungs. *Anat Rec.* 2009;292(1):113-122. doi:10.1002/ar.20747
  65. Brake MA, Ivanciu L, Maroney SA, Martinez ND, Mast AE, Westrick RJ. Assessing blood clotting and coagulation factors in mice. doi:10.1002/cpmo.61
  66. Mackman N, Tilley RE, Key NS. Role of the extrinsic pathway of blood coagulation in hemostasis and thrombosis. *Arterioscler Thromb Vasc Biol.* 2007;27(8):1687-1693. doi:10.1161/ATVBAHA.107.141911
  67. Grover SP, Mackman N. Tissue Factor: An Essential Mediator of Hemostasis and Trigger of Thrombosis. *Arterioscler Thromb Vasc Biol.* 2018;38(4):709-725. doi:10.1161/ATVBAHA.117.309846
  68. Kasthuri RS, Taubman MB, Mackman N. Role of tissue factor in cancer. *J Clin Oncol.* 2009;27(29):4834-4838. doi:10.1200/JCO.2009.22.6324

69. Palumbo JS, Talmage KE, Massari J V., et al. Tumor cell-associated tissue factor and circulating hemostatic factors cooperate to increase metastatic potential through natural killer cell-dependent and -independent mechanisms. *Blood*. 2007;110(1):133-141. doi:10.1182/blood-2007-01-065995
70. Rao LVM, Kothari H, Pendurthi UR. Tissue factor: Mechanisms of decryption. *Front Biosci - Elit*. 2012;4 E(4):1513-1527. doi:10.2741/e477
71. Yang X, Cheng X, Billiar TR, Han J, Correspondence BL. Bacterial Endotoxin Activates the Coagulation Cascade through Gasdermin D-Dependent Phosphatidylserine Exposure. *Immunity*. 2019;51:983-996.e6. doi:10.1016/j.immuni.2019.11.005
72. Shaw AW, Pureza VS, Sligar SG, Morrissey JH. The local phospholipid environment modulates the activation of blood clotting. *J Biol Chem*. 2007;282(9):6556-6563. doi:10.1074/jbc.M607973200
73. Spronk HMH, Ten Cate H, Van Der Meijden PEJ. Differential roles of Tissue Factor and Phosphatidylserine in activation of coagulation. *Thromb Res*. 2014;133(SUPPL. 1):S54-S56. doi:10.1016/j.thromres.2014.03.022
74. Bach R, Rifkin DB. Expression of tissue factor procoagulant activity: Regulation by cytosolic calcium. *Proc Natl Acad Sci U S A*. 1990;87(18):6995-6999. doi:10.1073/pnas.87.18.6995
75. Castillo Ferrer C, Berthenet K, Ichim G. Apoptosis – Fueling the oncogenic fire. *FEBS J*. November 2020;febs.15624. doi:10.1111/febs.15624
76. Schuster E, Taftaf R, Reduzzi C, Albert MK, Romero-Calvo I, Liu H. Better together: circulating tumor cell clustering in metastatic cancer. *Trends in Cancer*. 2021;7(11):1020-1032. doi:10.1016/j.trecan.2021.07.001

77. Cheung KJ, Ewald AJ. A collective route to metastasis: Seeding by tumor cell clusters. *Science (80- )*. 2016;352(6282):167-169. doi:10.1126/science.aaf6546
78. Unruh D, Horbinski C. Beyond thrombosis: The impact of tissue factor signaling in cancer. *J Hematol Oncol*. 2020;13(1):1-14. doi:10.1186/s13045-020-00932-z
79. Duda DG, Duyverman AMMJ, Kohno M, et al. Malignant cells facilitate lung metastasis by bringing their own soil. *Proc Natl Acad Sci U S A*. 2010;107(50):21677-21682. doi:10.1073/pnas.1016234107
80. Ortiz-Otero N, Clinch AB, Hope J, Wang W, Reinhart-King CA, King MR. Cancer associated fibroblasts confer shear resistance to circulating tumor cells during prostate cancer metastatic progression. *Oncotarget*. 2020;11(12):1037-1050. doi:10.18632/oncotarget.27510
81. Lu T, Oomens L, Terstappen LWMM, Prakash J. In Vivo Detection of Circulating Cancer-Associated Fibroblasts in Breast Tumor Mouse Xenograft: Impact of Tumor Stroma and Chemotherapy. *Cancers (Basel)*. 2023;15(4):1-16. doi:10.3390/cancers15041127
82. Wang J, Kwaan HC. The pathogenetic role of apoptosis in hypercoagulable states. *Hematology*. 2001;6(2):143-152. doi:10.1080/10245332.2001.11746565
83. Wang JG, Manly D, Kirchhofer D, Pawlinski R, Mackman N. Levels of microparticle tissue factor activity correlate with coagulation activation in endotoxemic mice. *J Thromb Haemost*. 2009;7(7):1092-1098. doi:10.1111/j.1538-7836.2009.03448.x
84. Aras O, Shet A, Bach RR, et al. Induction of microparticle- and cell-associated intravascular tissue factor in human endotoxemia. *Blood*. 2004;103(12):4545-4553. doi:10.1182/blood-2003-03-0713

85. Schmaier AA, Anderson PF, Chen SM, et al. TMEM16E regulates endothelial cell procoagulant activity and thrombosis. *J Clin Invest*. 2023;133(11). doi:10.1172/JCI163808
86. Bombeli T, Karsan A, Tait JF, Harlan JM. Apoptotic vascular endothelial cells become procoagulant. *Blood*. 1997;89(7):2429-2442. doi:10.1182/blood.v89.7.2429
87. Muhsin-Sharafaldine MR, Kennedy BR, Saunderson SC, et al. Mechanistic insight into the procoagulant activity of tumor-derived apoptotic vesicles. *Biochim Biophys Acta - Gen Subj*. 2017;1861(2):286-295. doi:10.1016/j.bbagen.2016.11.020
88. Muhsin-Sharafaldine MR, Saunderson SC, Dunn AC, Faed JM, Kleffmann T, McLellan AD. Procoagulant and immunogenic properties of melanoma exosomes, microvesicles and apoptotic vesicles. *Oncotarget*. 2016;7(35):56279-56294. doi:10.18632/oncotarget.10783
89. Muhsin-Sharafaldine MR, McLellan AD. Apoptotic vesicles: deathly players in cancer-associated coagulation. *Immunol Cell Biol*. 2018;96(7):723-732. doi:10.1111/imcb.12162
90. Zhang C, Yang Z, Zhou P, et al. Phosphatidylserine-exposing tumor-derived microparticles exacerbate coagulation and cancer cell transendothelial migration in triple-negative breast cancer. *Theranostics*. 2021;11(13):6445-6460. doi:10.7150/thno.53637
91. Grover SP, Hisada YM, Kasthuri RS, Reeves BN, MacKman N. Cancer Therapy-Associated Thrombosis. *Arterioscler Thromb Vasc Biol*. 2021;41(4):1291-1305. doi:10.1161/ATVBAHA.120.314378
92. Khalil J, Bensaid B, Elkacemi H, et al. Venous thromboembolism in cancer patients: An underestimated major health problem. *World J Surg Oncol*. 2015;13(1):1-17. doi:10.1186/s12957-015-0592-8
93. Khorana AA, Francis CW, Culakova E, Kuderer NM, Lyman GH. Thromboembolism is a leading cause of death in cancer patients receiving outpatient chemotherapy [10]. *J*

- Thromb Haemost.* 2007;5(3):632-634. doi:10.1111/j.1538-7836.2007.02374.x
94. Lima LG, Chammas R, Monteiro RQ, Moreira MEC, Barcinski MA. Tumor-derived microvesicles modulate the establishment of metastatic melanoma in a phosphatidylserine-dependent manner. *Cancer Lett.* 2009;283(2):168-175. doi:10.1016/j.canlet.2009.03.041
95. Jing H, Wu X, Xiang M, Wang C, Novakovic VA, Shi J. Microparticle Phosphatidylserine Mediates Coagulation : Involvement in Tumor Progression and Metastasis. 2023:1-29.
96. Sharma B, Kanwar SS. Phosphatidylserine: A cancer cell targeting biomarker. *Semin Cancer Biol.* 2018;52(September 2017):17-25. doi:10.1016/j.semcancer.2017.08.012
97. Budhu S, Giese R, Gupta A, et al. Targeting Phosphatidylserine Enhances the Anti-tumor Response to Tumor-Directed Radiation Therapy in a Preclinical Model of Melanoma. *Cell Rep.* 2021;34(2):108620. doi:10.1016/j.celrep.2020.108620
98. Wang W, Wu S, Cen Z, et al. Mobilizing phospholipids on tumor plasma membrane implicates phosphatidylserine externalization blockade for cancer immunotherapy. *CellReports.* 2022;41(5):111582. doi:10.1016/j.celrep.2022.111582
99. Utsugi T, Schroit AJ, Connor J, Bucana CD, Fidler IJ. Elevated Expression of Phosphatidylserine in the Outer Membrane Leaflet of Human Tumor Cells and Recognition by Activated Human Blood Monocytes. *Cancer Res.* 1991;51(11):3062-3066.
100. Riedl S, Rinner B, Asslaber M, et al. In search of a novel target - phosphatidylserine exposed by non-apoptotic tumor cells and metastases of malignancies with poor treatment efficacy. *Biochim Biophys Acta.* 2011;1808(11):2638-2645. doi:10.1016/j.bbamem.2011.07.026
101. Kaynak A, Davis HW, Kogan AB, Lee JH, Narmoneva DA, Qi X. Phosphatidylserine:

- The Unique Dual-Role Biomarker for Cancer Imaging and Therapy. *Cancers (Basel)*. 2022;14(10). doi:10.3390/cancers14102536
102. Nagata S, Suzuki J, Segawa K, Fujii T. Exposure of phosphatidylserine on the cell surface. *Cell Death Differ*. 2016;23(6):952-961. doi:10.1038/cdd.2016.7
103. Le DT, Rapaport SI, Rao LVM. Relations between factor VIIa binding and expression of factor VIIa/tissue factor catalytic activity on cell surfaces. *J Biol Chem*. 1992;267(22):15447-15454. doi:10.1016/s0021-9258(19)49554-9
104. Carson SD, Johnson DR. Consecutive enzyme cascades: Complement activation at the cell surface triggers increased tissue factor activity. *Blood*. 1990;76(2):361-367. doi:10.1182/blood.v76.2.361.bloodjournal762361
105. Carson SD, Archer PG. Tissue factor activity in hela cells measured with a continuous chromogenic assay and elisa reader. *Thromb Res*. 1986;41(2):185-195. doi:10.1016/0049-3848(86)90228-8
106. Tardáguila M, Mañes S. CX3CL1 at the crossroad of EGF signals relevance for the progression of ERBB2+ breast carcinoma. *Oncoimmunology*. 2013;2(9):8-10. doi:10.4161/onci.25669
107. Tang J, Chen Y, Cui R, et al. Upregulation of fractalkine contributes to the proliferative response of prostate cancer cells to hypoxia via promoting the G1/S phase transition. *Mol Med Rep*. 2015;12(6):7907-7914. doi:10.3892/mmr.2015.4438
108. Mao P, Smith L, Xie W, Wang M. Dying endothelial cells stimulate proliferation of malignant glioma cells via a caspase 3-mediated pathway. *Oncol Lett*. 2013;5(5):1615-1620. doi:10.3892/ol.2013.1223
109. Chaurio R, Janko C, Schorn C, et al. UVB-irradiated apoptotic cells induce accelerated

- growth of co-implanted viable tumor cells in immune competent mice. *Autoimmunity*. 2013;46(5):317-322. doi:10.3109/08916934.2012.754433
110. Medina CB, Mehrotra P, Arandjelovic S, et al. Metabolites released from apoptotic cells act as tissue messengers. *Nature*. March 2020:1-6. doi:10.1038/s41586-020-2121-3
111. Kumar S, Calianese D, Birge RB. Efferocytosis of dying cells differentially modulate immunological outcomes in tumor microenvironment. *Immunol Rev*. 2017;280(1):149-164. doi:10.1111/imr.12587
112. Stanford JC, Young C, Hicks D, et al. Efferocytosis produces a prometastatic landscape during postpartum mammary gland involution. *J Clin Invest*. 2014;124(11):4737-4752. doi:10.1172/JCI76375
113. Li F, Huang Q, Chen J, et al. Apoptotic cells activate the “phoenix rising” pathway to promote wound healing and tissue regeneration. *Sci Signal*. 2010;3(110):1-10. doi:10.1126/scisignal.2000634
114. Atsumi GI, Tajima M, Hadano A, Nakatani Y, Murakami M, Kudot I. Fas-induced arachidonic acid release is mediated by Ca<sup>2+</sup>- independent phospholipase A2 but not cytosolic phospholipase A2, which undergoes proteolytic inactivation. *J Biol Chem*. 1998;273(22):13870-13877. doi:10.1074/jbc.273.22.13870
115. Castellone MD, Teramoto H, Williams BO, Druey KM, Gutkind JS. Medicine: Prostaglandin E2 promotes colon cancer cell growth through a Gs-axin-β-catenin signaling axis. *Science (80- )*. 2005;310(5753):1504-1510. doi:10.1126/science.1116221
116. Werfel TA, Elion DL, Rahman B, et al. Treatment-induced tumor cell apoptosis and secondary necrosis drive tumor progression in the residual tumor microenvironment through MERTK and IDO1. *Cancer Res*. 2019;79(1):171-182. doi:10.1158/0008-

5472.CAN-18-1106

117. Zhou Y, Fei M, Zhang G, et al. Blockade of the Phagocytic Receptor MerTK on Tumor-Associated Macrophages Enhances P2X7R-Dependent STING Activation by Tumor-Derived cGAMP. *Immunity*. 2020;0(0). doi:10.1016/j.immuni.2020.01.014
118. Qin J, Zhang Z, Fu Z, et al. The UDP/P2y6 axis promotes lung metastasis of melanoma by remodeling the premetastatic niche. *Cell Mol Immunol*. March 2020:1-3. doi:10.1038/s41423-020-0392-0
119. Giampazolias E, Zunino B, Dhayade S, et al. Mitochondrial permeabilization engages NF- $\kappa$ B-dependent anti-tumour activity under caspase deficiency. *Nat Cell Biol*. 2017;19(9):1116-1129. doi:10.1038/ncb3596
120. Hejna M, Raderer M, Zielinski CC. Inhibition of metastases by anticoagulants. *J Natl Cancer Inst*. 1999;91(1):22-36. doi:10.1093/jnci/91.1.22
121. Najidh S, Versteeg HH, Buijs JT. A systematic review on the effects of direct oral anticoagulants on cancer growth and metastasis in animal models. *Thromb Res*. 2020;187(October 2019):18-27. doi:10.1016/j.thromres.2019.12.022
122. Mosarla RC, Vaduganathan M, Qamar A, Moslehi J, Piazza G, Giugliano RP. Anticoagulation Strategies in Patients With Cancer: JACC Review Topic of the Week. *J Am Coll Cardiol*. 2019;73(11):1336-1349. doi:10.1016/j.jacc.2019.01.017
123. Górnicki T, Bułdyś K, Zielińska D, Chabowski M. Direct-Acting Oral Anticoagulant Therapy in Cancer Patients—A Review. *Cancers (Basel)*. 2023;15(10):1-17. doi:10.3390/cancers15102697
124. Tan YS, Lei YL. Generation and culture of mouse embryonic fibroblasts. *Methods Mol Biol*. 2019;1960:85-91. doi:10.1007/978-1-4939-9167-9\_7